Fish and Shellfish Immunology 154 (2024) 109992

Contents lists available at ScienceDirect

Fish and Shellfish Immunology

journal homepage: www.elsevier.com/locate/fsi

Full length article

Cell death induced by *Lepeophtheirus salmonis* labial gland protein 3 in salmonid fish leukocytes: A mechanism for disabling host immune responses

Helena Marie Doherty Midtbø [a,*], Andreas Borchel [a], H. Craig Morton [b], Richard Paley [c], Sean Monaghan [d], Gyri Teien Haugland [a], Aina-Cathrine Øvergård [a]

[a] Department of Biological Sciences, University of Bergen, P.O. Box 7803, NO-5020, Bergen, Norway
[b] Institute of Marine Research, P.O. Box 1870 Nordnes, NO-5817, Bergen, Norway
[c] Centre for Environment, Fisheries and Aquaculture Science (Cefas), The Nothe, Barrack Road, Weymouth, DT4 8UB, United Kingdom
[d] Institute of Aquaculture, University of Stirling, Stirling, United Kingdom

ARTICLE INFO

Keywords:
Arthropod
Copepod
Host-parasite interaction
Immune modulation
Transcriptomics
Cell sorting
Skin histology

ABSTRACT

The salmon louse (*Lepeophtheirus salmonis*) is an ectoparasite feeding on mucus, skin, and blood of salmonids. On parasitised fish erosions and, at later lice stages, ulcerations appear at the louse feeding site. In susceptible species like Atlantic salmon (*Salmo salar*) with a limited rejection of lice, only a mild inflammatory response with minor influx of immune cells is seen at these lesions, as the salmon louse secrete proteins that can dampen immune responses. In a previous study, *Lepeophtheirus salmonis* labial gland protein 3 (LsLGP3) was suggested to dampen cellular responses, and the present study aimed at increasing our understanding of its mode of action. LsLGP3 was found to be secreted on to the host skin, and both *in vivo* and *in vitro* experiments were performed to elucidate its function. Histological analysis of the louse attachment site revealed an epidermal and dermal influx of mainly macrophages and granulocytes after 5 days post infestation. The immune cell influx was deeper in the dermis throughout the louse infestation, and LsLGP3 may be involved in dampening this response. Enriched populations of Atlantic salmon B-cells, T-cells, granulocytes, and monocytes were exposed to recombinant LsLGP3 (recLGP3) *in vitro*, resulting in a significant decrease in cell viability compared to non-exposed controls. An apoptotic cell morphology with "beads-on-a-string" like protrusions was seen in all leukocyte cell fractions after recLGP3 exposure, but not in erythrocytes or keratocytes. A decreased viability was also detected in pink salmon leucocytes, which was not in leucocytes from non-salmonid species. These functional insights suggest that LsLGP3 specifically induces apoptosis of salmonid leukocytes and is likely a key protein secreted by the lice that disables the Atlantic salmon ability to mount an adequate immune response towards the salmon louse. *In vivo* LsLGP3 knock down studies indicated that the effect is localised primarily at the lice feeding site, without affecting immune cells that are not situated adjacent to the lice-inflicted lesion. The findings from this study could significantly aid in the development of new immune based anti-salmon louse prophylactic measures and treatments.

1. Introduction

The salmon louse (*Lepeophtheirus salmonis*) is a marine copepod ectoparasite infesting the skin of salmonid fish. Here, the louse feeds on host mucus, skin, and blood, causing mechanical damage seen as erosions and light ulcers [1–5]. High levels of parasites can be harmful to smaller fish, causing chronic stress that increases their susceptibility to other diseases, and disrupt their osmotic balance [5–8]. High salmon louse numbers in farmed areas are suggested to negatively impact wild Atlantic salmon and sea trout (*Salmo trutta)* populations [9–11]. Consequently, measures have been implemented to manage and control salmon louse numbers on farmed fish [12,13]. The current delousing methods in use, however, either have a low efficacy, risk of resistance-development or cause problems with fish health and welfare [14,15]. Therefore, there is a need for new and sustainable methods for maintaining low lice numbers in salmon farms, such as immune based

* Corresponding author.
E-mail address: Helena.midtbo@uib.no (H.M.D. Midtbø).

https://doi.org/10.1016/j.fsi.2024.109992
Received 29 April 2024; Received in revised form 25 October 2024; Accepted 28 October 2024
Available online 30 October 2024

anti-salmon louse prophylactic measures and treatments. To obtain this, more knowledge about the host-parasite interaction and salmon louse biology is needed.

The life cycle of the salmon louse consists of eight developmental stages separated by moults [16,17]. After two free living planktonic stages (nauplius I and II), the copepodid stage can attach to and feed off the fish mucus and epidermis and cause superficial wounds [3,16,18,19]. This enables the louse to moult to the chalimus stage, where it increases in size and causes more damage to its host [3]. The chalimus further moults into the pre-adult and adult stages, where the louse inflicted wounds extends into the dermis as the lice starts blood feeding [4,19,20]. In susceptible species like Atlantic salmon (*Salmo salar*) and rainbow trout (*Oncorhynchus mykiss*), lice clearance is minimal, even though an influx of immune cells are observed in the dermis [4,19–21]. The number of immune cells attracted to the point of attachment is, however, not very prominent, and only a modest early increase in transcripts encoding immune cell markers such as *non-specific cytotoxic cell receptor protein 1 (nccrp1)* and *cd8a* are seen [19,22]. Interestingly, a significant downregulation of transcripts related to the adaptive immune response has been observed in Atlantic salmon and rainbow trout skin at adult louse attachment site [19,22]. Thus, the louse seems to dampen host immune response in susceptible salmonids to avoid clearance. In contrast, juvenile pink salmon *(Oncorhynchus gorbuscha)* is one of the least susceptible salmonid species and mostly clears off the infestation at the copepodid or chalimus I stage [23–25]. In pink salmon, lesions at the louse attachment site are seen as ulcerative necrosis, haemorrhage, and mucosal and dermal leukocyte infiltration [26]. In Coho salmon *(Oncorhynchus kisutch)*, also resistant to the salmon louse, dermal mast cells and epidermal macrophages, neutrophils and lymphocytes are seen at the louse attachment site, followed by keratocyte hyperplasia [27,28]. As hyperplasia followed by fibrosis is commonly induced in Atlantic salmon skin towards louse remnants [3], it seems that live salmon lice prevent Atlantic salmon to mount an adequate response to clear off the louse infestation.

The salmon louse was recently found to dampen immune responses through protein secretion from louse exocrine glands, more specifically the labial glands [29,30]. Labial gland proteins are secreted through ducts ending next to the mandible teeth that are used for feeding [31,32]. Thus, labial gland proteins from the salmon louse are proposed to be deposited onto the lice feeding site to enable a dampening of host responses [29,30,32]. As of now, 15 labial gland proteins are identified, and most of these proteins seem to be important for host settlement as the labial gland gene expression is initiated once the copepodid become infective prior to host settlement [29,30]. There are, however, two transcripts that are induced as a response to host settlement, namely *Lepeophtheirus salmonis* labial gland apyrase 7 (LsLGA7) and *Lepeophtheirus salmonis* labial gland protein 3 (LsLGP3) [29]. LsLGP3 is a relatively small (18 kDa) positively charged protein having labial gland expression that increases as the lice develops into the more virulent adult stages [30]. As recombinant LsLGP3 (recLGP3) decreased the transcript level of *igd, igt, cd8α,* and *ifng* in Atlantic salmon head kidney leukocytes, LsLGP3 was suggested to dampen cellular responses through an unknown mode of action. The present study therefore aimed to understand how LsLGP3 may dampen cellular responses and its specificity to different fish species and cell types. *In vivo* functional knock-down (KD) in lice followed by transcriptomic analysis of host responses towards KD lice, and *in vitro* viability measurements of recLGP3-exposed leukocytes separated in different cell populations and isolated from different fish species were carried out to elucidate the mechanism behind LsLGP3-induced cell dampening.

2. Materials and methods

2.1. In vivo experiments

2.1.1. Rearing and source of L. salmonis

The lab strain LsGulen of *L. salmonis salmonis* was used and reared on farmed Atlantic salmon in 1 x 1 flow through tanks at 34 ppt NaCl, 9 ± 0.5 °C, 12:12 light cycle, and nauplii were obtained from hatching eggs and kept in single wells in a flow through system according to Hamre et al. (2009), both at the wet lab facility of the University of Bergen, Norway.

2.1.2. Rearing conditions and histology

Atlantic salmon with an average weight of 350 ± 48 g were acclimatised for 14 days in 1 × 1 m flow through tanks at 12 °C, 34 ppt NaCl and 12:12 light cycle at the wet lab facility of the University of Bergen, Norway. The fish were daily hand fed with Nutra Olympic 4.0 mm (Skretting). They were infested with 100 copepodids/fish and scaled skin samples for histology were taken 3-, 5- and 7-days post infestation (dpi), and in a separate experiment under the same conditions, samples were taken 12 days post infestation. In a third experiment, the infestation pressure was lowered to 50 copepodids/fish due to animal welfare and higher virulence of pre-adult/adult lice, and fish kept at 9.3 °C could thereby be left for 51 dpi when scaled skin samples for histology were taken. Specimens were fixed by overnight immersion in a mixture of 0.9 % formaldehyde, 2.3 % glutaraldehyde, 4 % (w/v) sucrose in PBS (380 mOsm/L) with the pH adjusted to 7.35. Following this, the specimen was dehydrated using a graded ethanol series (50, 70, 80, 90, 96 %). The Technovit 7100 solution (Heraeus Kulzer Technique) was used according to the manufacturer's recommendations for 6-h pre-infiltration, 12-h infiltration and embedding. The specimens were sectioned (2 μm) using a microtome (Leica RM 2165) and stained with 1 % Toluidine blue and 0.1 % sodium borate for 1 min and rinsed in running tap water. Toluidine blue is an acidophilic, thiazine metachromatic dye, which stain nucleic acids and most protein in blue, while proteoglycans in cartilage matrix and mucins display a purple to red colour [33]. The stained sections were mounted using DPX new (Merck).

2.1.3. RNA interference and infestation

RNA interference (RNAi) studies of LsLGP3 knock-down in the *L. salmonis* strain LsLGulen were done, followed by an infestation trial on Atlantic salmon at the wet lab facility of the University of Bergen, Norway. Double stranded RNA (dsRNA) was produced using MEGAscript RNAi Kit (Ambion) according to the supplier's protocol, using the primers listed in Table 1. Around 60–100 salmon louse nauplius I larvae from the same egg string were soaked in 20 ng/μl LsLGP3 dsRNA in 150 μl sea water overnight, as previously described [34]. The control group received elution buffer, without dsRNA. All animals within one treatment group were pooled and kept in flow through incubators until at least 2 days after moulting to copepodids. Atlantic salmon with an average weight of 130 ± 32 g were kept in 50 L single fish tanks with racks of three fish tanks on the same water supply, at 12 °C, 34 ppt, 12:12 light cycle and acclimatised for 14 days, as previously described [35]. The fish were daily hand fed with Nutra Olympic 4.0 mm (Skretting) and were closely monitored, ensuring that they showed a good appetite and little signs of stress. There were four treatment groups (n = 8): an untreated group, fish infested with control lice and fish infested with knock down (KD) lice for 5 and 7 days. The lice infestation was done after changing to individual water in – and outlet for each tank. The water level was lowered to a minimum, keeping the fish covered with water whilst maintaining normal water flow and adding 150 cops/fish. Tanks returned to normal levels within 5–10 min and non-attached copepodids were flushed out of the system. Five hours post infestation regular waterflow was reestablished. Scaled skin samples were taken 5- and 7-days post infestation at the lice infestation site (Inf+) and at non-infested areas (Inf-), and from comparable sites on the

Table 1
Primers used to create LsLGP3 dsRNA for RNAi experiments and target LsLGP3 by qPCR.

Gene	Forward (5'→3')	Reverse (5'→3')	Use
LsLGP3	CCAGTGGGCTCCAATCCTAGTGAA	AGTTTGGGCTGTTGTTCCGGTT	RNAi
LsLGP3	TCAAGAAGGATTTGAAAAGTTGACGAATG	TGCCCGATTGTTCCATAATTCCGTT	qPCR

uninfested fish (Uninf).

In addition, adult lice were injected with dsRNA in a separate experiment, and the fish were infested by gently putting seven adult female lice and four adult male lice on a piece of moisted paper and gently applying the inverted paper behind the dorsal fin on anesthetised fish. The fish had a weight of 216 ± 50 g. There were three treatment groups (n = 8): an uninfested group, fish infested with control lice and fish infested with KD lice for 21 days. The experimental conditions and sampling were the same as above, but in addition, head kidney (HK) samples were taken.

2.1.4. RNA sequencing and transcriptome analyses

The HK and scaled skin samples were collected and submerged in RNA-later (Life Technologies), kept overnight at 4 °C and then stored at −20 °C. Total RNA was isolated by combining Tri reagent (Sigma Aldrich) and RNeasy micro kit (Qiagen) as previously described [36], with on-column DNase treatment. Extracted RNA was kept at −80 °C until further use. The LsLGP3 KD efficiency was analysed as previously described (Supplementary Fig. 1) [30]. Five fish from each group were randomly selected for transcriptomic analysis by Illumina NovaSeq6000 Sequencing at the Genomics Core Facility, University of Bergen. Total RNA quality was checked by Agilent Bioanalyzer (RIN >9) and quantified using Qubit. Libraries were prepared using Illumina Stranded mRNA, Ligation kit. The library was quantified using Illumina MiSeq Nano flowcell and quality checked on Agilent TapeStation. The samples were loaded on NovaSeq S1-flow cells. Sequencing parameters for Illumina NovaSeq6000: 2x100bp paired end reads. Raw reads were deposited in the NCBI Short Reads Archive and are accessible with bio project accession number: PRJNA1089937.

The obtained reads were mapped, without further filtering, to the *Salmo salar* transcriptome, derived from genome Ssal_v3.1, using Salmon (version 1.10.1) [37]. The procedure was performed on the usegalaxy.eu web server [38]. The *S. salar* genome (Ssal_v3.1) was used as to create a decoy database. For samples with attached salmon lice (chalimi), the decoy database was supplemented with the *L. salmonis* transcriptome and genome (LSalAtl2s), to filter out reads originating from the attached lice. Transcriptomes and genomes were obtained from Ensembl (release 110) and Ensembl Metazoa (release 56) [39,40]. The mapping rates were between 72 and 79 %.

The next steps were performed in R [41]. The count files were prepared for differential expression analysis using tximport, and analysed with DESeq2 [42,43]. Individual analyses were run for the different samples: head kidney, skin with adult lice, skin with chalimus 5 dpi and skin with chalimus 7 dpi. For each comparison, pre-filtering based on the numbers of mapped reads was performed. Genes with less than 10 mapped reads in at least five samples were discarded. Several models were used to identify those genes which were differentially regulated under the skin between fish infested with control lice and KD lice. In the first model, the fold changes between KD and Ctrl were calculated for the Inf+ and Inf-groups, respectively. These fold changes were shrunk using the apeglm method [44]. The second model looked for interactions between the sampling site (Inf+/Inf-) and the louse state (KD/Ctrl). The third model accounted also for the individual fish, looking for "Group-specific condition effects, individuals nested within groups", as described in the Bioconductor DeSeq2 manual [42]. The threshold for the false discovery rate to determine significantly differentially expressed genes was set to 0.05. For visualisation of normalised counts, the DESeq2 "counts" function with activated normalisation which divides the counts by the size factors or normalisation factors was employed.

2.1.5. LsLGP3 identification by LC/MS-MS

Atlantic salmon were reared according to section 2.1.1, and adult female lice were picked off the fish, and skin samples taken directly underneath the adult lice, and away from attachment site. Samples enriched for labial gland were taken by cutting the area around the mouth tube containing the labial gland. The specimen was homogenised directly in 4 x Laemmli sample buffer with β-mercaptoethanol (BioRad) using a steel bead and a TissueLyser (Qiagen). RecLGP3 described in section 2.2.4, was included as a control. The specimen was boiled (95 °C) for 5 min, and the proteins were separated on a stain-free 4–20 % SDS-PAGE gel (BioRad) and stained with Coomassie blue (BioRad). Bands at approx. 10–15 kDa and 15–22 kDa were cut out. For protein identification by LC/MS-MS, these samples were run on an Orbitrap Exploris 480 (ThermoFisher) at the proteomics unit at the Proteomics Core Facility, University of Bergen. The peptides were mapped to *S. salar* (Uniprot) and *L. salmonis* (LsSalAtl2s) proteome and identified in Proteome Discoverer 2.5 (PD2.5) from Thermo Fisher Scientific. The false discovery rate was low in the samples for *L.salmonis*. In the samples taken from Atlantic salmon skin underneath adult lice, for the detected LsLGP3 peptide a BLAST search against the *S. salar* and *L.salmonis* proteome was performed.

2.2. In vitro experiments

2.2.1. Fish maintenance for fish used in in vitro experiments

All fish were reared in 500 L flow through tanks unless otherwise specified, with a salinity of 34.5 ppt NaCl at 9 ± 0.5 °C, 12:12 light cycle and were fed daily. They were all acclimatised to the tank conditions for at least 14 days prior to sampling.

Atlantic salmon (Benchmark Genetics, Iceland) were reared at the facilities of The Industrial and Aquatic Laboratory (ILAB), Bergen, Norway and were fed with Nutra Olympic 4.0 mm (Skretting). Several Atlantic salmon batches were used in the experiments, ranging from 500 to 1200 g. In each individual experiment the fish were from the same tank and batch and had similar weights (± 10 %).

Fertilised pink salmon eggs were collected in the Dale River in Western Norway in the autumn of 2021. They were reared at the wet lab facilities of the University of Bergen, Norway, and feed with Nutra Olympic 2.0 mm (Skretting). At the sampling time, the fish were between 250 and 450 g, with no gonadal development (<1 g), n = 4.

Lumpfish (*Cyclopterus lumpus*) (Vest Aqua Base AS, Fitjar, Norway) and Atlantic cod (*Gadus morhua*) (Nofima, Tromsø, Norway) were reared at the facilities of ILAB, and fed with Amber Neptun 5.0 mm (Skretting). At sampling time lumpfish were ≈800 g, n = 4 and Atlantic cod were ≈2000 g, n = 3. Atlantic cod were reared in 2500 L flow through tanks.

Coho salmon were received as embryos in the "eyed" stage from the Quinsam River Hatchery, British Columbia, into the biosecurity facilities at the Centre for Environment, Fisheries and Aquaculture Science (Cefas), Weymouth, England under lifelong quarantine. The fish were hatched and reared through 50L and 500L tanks in freshwater, then smolted and transferred to seawater for further on-growing in 1000L tanks. Rearing temperature and light regime varied through different life stages and ranged from 8 to 15 °C and from 6:18hr (day: night) through 12:12 to 18:6 respectively with 150–200 lux at water surface. Fish were fed with a range of diets according to life stage comprising Nutra plus 00 (Skretting), Inicio plus 0.8, 1.1 and 1.5 (Biomar), Alltech Star Alevin 2.0 (Coppens), Orbit Intro 2.0 and 3.0 (Biomar) and Alltech

supreme 3.0 (Coppens). At sampling, the fish were in seawater at 10 °C with an average weight of 250 g, n = 4.

2.2.2. Leukocyte isolation

The fish were euthanized by a sharp blow to the head. Peripheral blood was gently drawn from *Vena caudalis* using a syringe, and immediately transferred to heparin containers. The blood was diluted 1:3, with supplemented L-15 media (2 % FBS, 0,5 % Ampicillin, 10 U ml^{-1} Heparin). Peripheral blood leukocytes (PBLs) were isolated as describe by Pettersen et al. [45], by using a discontinuous Percoll (Cytiva) gradient, where 4 mL of Percoll with a density of 1075 g ml^{-1} overlaid with a 3 mL Percoll with a density of 1060 g ml^{-1}. The gradient was centrifuged at 400 x rcf 4 °C for 40 min (Beckman GPR Centrifuge), and the leukocyte fraction was collected at the density layer interface. The leukocytes were washed twice in PBS 380 mOsm/L with 10 U ml^{-1} Heparin and centrifuged at 200 x rcf, 4 °C for 10 min. Isolated leukocytes were resuspended in 1 ml supplemented L-15 media and kept on ice. The viability and cell count were analysed using CASY-TT (Inovatis). Only leukocyte fractions with a cell viability above 95 % were used.

2.2.3. Cell sorting

Leukocytes were incubated in 6 well plates (1 x 10^7 cells per well) overnight (16 °C) in supplemented L-15 media (10 % FBS, 0.5 % Ampicillin, 10 U ml^{-1} Heparin). The media was taken off and used to gently wash the wells. The non-adherent cells from the media were kept on ice. The plates were washed with PBS and treated with trypsin and collected as the enriched population for monocytes.

The non-adherent leukocytes were washed in PBS +0.5 % BSA. Thereafter, non-adherent leukocytes were incubated with 1:200 diluted Anti-Salmonid Ig (H), FITC, (Clone IPA5F12, Cat no. 177-CLF004F, Cedarlane) at a cell density of 5 x 10^6 in PBS +0.5 % BSA in the dark (on ice, 30 min, gentle shaking). The cells were washed with PBS, 0.5 % BSA, 25 mM EDTA 3 times (200 x rcf, 10 min, 4 °C). The leukocytes were sorted in BD FACSymphony S6 flow cytometer (Flow Cytometry Core Facility, University of Bergen). IgM^+ - FITC cells were sorted by fluorescence into one fraction. The remaining lymphocytes were sorted by gating, obtaining an enriched population of T-cells and non-specific cytotoxic cells (NCC) low in granularity (low SSC) and size (low FSC), and an enriched population of granulocytes high in granularity (high SSC).

2.2.4. Heterologous expression of LsLGP3

RecLGP3 was produced as described in Øvergård et al. [30]. Briefly, *E. coli* MC1061 cells were transformed with expression vector p1, encoding LsLGP3 without signal peptide. Expression was induced with 0.1 % L-arabinose (Sigma) and the cells were incubated over-night at 20 °C, shaking at 250 rpm. Soluble LsLGP3 was purified with a Ni-NTA Fast Start kit (Qiagen) according to the supplier's instruction, and the buffer was exchanged with 1 x PBS using a Pierce Protein Concentrator, 3K MWCO (Thermo Scientific). The concentration was measured on a Nanodrop Spectrophotometer (A280 nm). The protein was stored at 4 °C over-night and used the following day, to avoid precipitation and to ensure an active protein.

recLGP3 mutations were made by changing positively charged amino acids to negatively charged amino acids in two regions which seemed to have an outer loop in the structure as predicted by AlphaFold [46]. Construct one (AΔLGP3) R79E; R83E; R84E, construct two (BΔLGP3) R121E; K122E and construct three (ABΔLGP3) combined all mutations R79E; R83E; R84E; R121E; K122E. Numeration of amino acids are based on the mature protein after signal peptide cleavage. Constructs of mutant LGP3 was produced by GenScript in the pET-15b vector and transformed in *E. coli* BL21 cells. The cells were grown in LB medium, and the expression was induced with IPTG at OD 0.8. The remaining procedure was done as described for recLGP3.

2.2.5. Cell staining

Cytospin preparations of the four enriched populations of leukocytes were prepared from 100 µl cell suspension of 1 x 10^6 cells ml^{-1} at 1000 rpm, 3 min (Shandon Cytospin III cytocentrifuge) and dried overnight. Due to low number of adherent cells (enriched for monocytes), only 2 x 10^5 cells were added.

Myeloid peroxidase (MPO) production was measured by staining to visualise cell population purity. The cytospin slides were fixed in 10 % (v/v) formaldehyde and 90 % (v/v) ethanol for 30 s and washed in running tap water and dried. The slides were incubated with diaminobenzidine staining solution prepared from SIGMAFAST DAB tablets (Sigma) for 30 min, rinsed in running tap water and mounted.

For nuclear staining, the cytospin slides were fixed using methanol and stained by dipping the slides eight times in Tetrabromfluorecein Disodium salt followed by Methylthionine chloride solution from ColorRapid (Tektron). The cytospin slides were examined using a Zeiss Axioscope A1.

2.2.6. In vitro recLGP3 exposure of peripheral blood leukocytes

Leukocytes were isolated as described in section 2.2.2. For all experiments, leukocytes from each fish were transferred to flow cytometry polystyrene tubes with a concentration of 5 x 10^5 cells per tube. Except for propidium iodide assay, leukocytes were plated in 48 well cell culture plates with a density of 2 x 10^6 (ThermoFisher). Leukocytes were exposed to 1 x PBS (control) or 25, 50, 100 or 200 µg recLGP3 in PBS, in a total volume of 300 µl. For the remaining experiments all populations were exposed to 112 µg recLGP3 in 300 µl. Except for in the experiment comparing coho and Atlantic leukocytes, where 56 µg and 112 µg recLGP3 with 2.5 x 10^5 cells per tube, in a total volume of 150 µl was used. The cells were incubated at 16 °C for 6 h for viability assay measured by CASY and 2 h staining with propidium iodide (2.2.7), and for 1 h for scanning electron microscopy (SEM) (2.2.8).

2.2.7. Cell viability measurement

After recLGP3 exposure, the viability of leukocytes was measured by resuspending the cells and using a CASY-TT (Inovatis) cell counter, where the percentage of viable cells was measured. For coho salmon leukocytes, the viability was determined by staining the cells with trypan blue (Sigma-Aldrich) and counting the non-stained viable leukocytes using a hemacytometer prior to recLGP3 exposure and after 6 h LGP3 exposure. The viability for Atlantic salmon leukocytes was also determined by propidium iodide staining (Sigma) and detected by an inverted fluorescent microscope (Leica DM IL LED). Extracellular DNA was stained by SYTOX Green (Invitrogen) and detected by an inverted confocal microscope (Olympus FV3000) and monitored every 15 min for 2 h.

When analysing unsorted PBLs, three biological replicates were used and for enriched leukocyte cell populations, five biological replicates were used, and all experiments were repeated twice. For the LsLGP3 mutational analysis, three biological replicates were used, and the experiment was repeated twice. For the species comparison, the experiments were done on separate days due to fish availability. At least one Atlantic salmon control was included in each experiment, the following number of biological replicates were used: Atlantic salmon:7, pink salmon: 4, lumpfish 4, Atlantic cod: 3, coho salmon: 4.

2.2.8. Scanning electron microscopy

Enriched cell populations of Atlantic and coho salmon leukocytes and Atlantic salmon skin explant were exposed to recLGP3 for 1 and 6 h, respectively, and fixed by overnight immersion in a mixture of 0.9 % formaldehyde, 2.3 % glutaraldehyde, 4 % (w/v) sucrose in PBS (380 mOsm/L) and with the pH adjusted to 7.35. The cells were washed in PBS prior to post-fixation with 1 % OsO_4 for 1 h. The specimen was washed with water and then dehydrated with ethanol (60, 90, 2 × 100 %) and dried on a glass coverslip at 37 °C overnight. The coverslip was mounted on stubs with carbon conductive tape and coated with gold-

palladium using Emitech K550X sputterer (Emitech, Ashford). The specimen was further studied using FEI Quanta 450 SEM at the ELMILAB at the University of Bergen.

2.2.9. Intracellular calcium measurements

PBLs were exposed to recLGP3 for 1, 2, 5, 10, 15, 30, 45, 60 and 75 min and stained with Calbryte 520 a.m. (AAT Bioquest). The cells were resuspended, and the fluorescence was detected using BD FACSCalibur, excitated at 488 nm, detected with a 530/30 band pass filter. Hypochlorous acid (200 μM) and PBS were used as a positive and negative control, respectively.

2.2.10. Statistics

Statistical analyses for *in vitro* experiments were performed in GraphPad Prism 10.1.1 (GraphStat). Unpaired, parametric *t*-test with Welch's correction was used to calculate statistical significance. Threshold p-value was set to 0.05.

2.3. Ethics statement

All experimental procedures were performed in strict accordance with Norwegian animal welfare legislation and guidelines at an approved animal facility. The lice infestation studies were carried out with approval from the Ethics committee of Norwegian Food Safety Authority (permit ID: 26020) following ARRIVE guidelines. In the remaining *in vitro* experiments, fish were reared under optimal rearing conditions and were killed by a sharp blow to the head, which is an appropriate procedure under Norwegian law (FOR-2015-06-18-761 §16). Tissues and cells were harvested from dead fish and does not require ethical approval under Norwegian law (FOR-2015-06-18-761 §6).

3. Results

3.1. L. salmonis produce the deduced LsLGP3 and secrete it onto the host skin

Labial gland expression of LsLGP3 protein has not been confirmed previously, nor if the labial gland proteins are in fact deposited onto the host skin. To determine whether *LsLGP3* is translated into protein and secreted onto the host, salmon louse samples enriched for labial gland in addition to skin tissue at the adult louse infestation site were dissected. The presence of LsLGP3 protein in samples enriched for labial gland was detected by LC-MS/MS in two different SDS-PAGE bands at ≈10–19 and ≈ 20–30 kDa, where 12–13 unique LsLGP3 peptides were detected (Supplementary file 1). Most LsLGP3 peptides in the sequence were detected with relatively high sequence coverage (62 %) of the deduced mature protein. Additionally, peptides from the *Lepeophtheirus salmonis* labial gland serine protease 1 (LsLGSP1) and labial gland protein 2 (LsLGP2) were detected. However, in SDS-PAGE bands analysed by LC-MS/MS from salmon skin samples taken underneath adult lice, only twenty salmon louse proteins were identified by LC-MS/MS in total (Supplementary file 1). Among them were LsLGP3, with only one unique peptide. Notably this peptide had 100 % sequence coverage and is not found in other salmon louse or salmon proteins, nor in the sample taken at non-attachment site.

3.2. Salmon louse infestations induce both an epidermal and dermal immune cell influx

As the histopathological examination around the salmon louse mouth tube on Atlantic salmon scaled skin infested with juvenile life stages of salmon louse are scarce, our initial objective was to investigate the location and influx of immune cells towards copepodid, chalimus I and II, and adult lice stages prior to conducting functional KD studies. A gradual increase in lesions was seen from the copepodid stage onwards, where predominantly erosions were observed in the analysed larval stages (3, 5, 7 and 12 dpi) while a more intact epidermal surface was observed at the adult lice attachment sites at 51 dpi (Fig. 1). Skin samples taken at 3 dpi showed no influx of immune cells (Fig. 1A and B), whereas cells mainly with a polymorphonuclear-like morphology started to appear in both the epidermis and dermis at the lice feeding site from 5 dpi and onwards (Fig. 1C and D). At 5 dpi, if immune cells were present, they were mainly seen in the dermis covering the scale to which the louse was attached, and not in deeper layers of the stratum spongiosum. The immune cells were not found to be restricted to directly underneath the louse, extending a bit laterally and anteriorly to the lice, with fewer immune cells seen adjacent to the erosion. Cell debris were also seen here. At later time points, a more pronounced, albeit still a minor, immune cell influx was observed underneath the lice at both 7 and 12 dpi, both in the epidermis and dermis surrounding the lice feeding site (Fig. 1E, F, H, I). However, fewer immune cells were seen in the dermis directly underneath the mouth tube at these time points. At 7 dpi, the dermal immune cell influx was still mainly restricted to the dermis covering the scale at louse attachment site, while immune cells could be seen in deeper layers of the stratum spongiosum underneath chalimus II lice (12 dpi). At the adult stage, 51 dpi, ulcerations, epidermal oedema, keratocyte degeneration and possible hyperplasia, along with a much more evident infiltrations of immune cells in the stratum spongiosum were observed (Fig. 1G–J, K). Interestingly, epidermal changes were more evident close to the dermis, while the superficial epidermal cells maintained intact cell junction and showed no degeneration. In the area which is proposed to be beneath the adult louse mouth tube, a localised epidermal and dermal grazing is observed (Supplementary Fig. 1).

3.3. LsLGP3 is implicated in a decrease in immune related genes at the louse infestation site

Attempts have previously been made to analyse the function of LsLGP3 by the induction of *LsLGP3* KD in adult lice that were allowed to infest Atlantic salmon with a subsequent measurement of the localized skin immune response [30]. Despite a 4-day exposure to KD and control lice, no significant difference was observed in the transcript levels of selected immune genes between the groups. As the duration and the number of immune genes analysed in the previous study might have been suboptimal to elucidate any alteration in cellular response, further KD experiments were conducted in the present study. As LsLGP3 expression is initiated in the copepodid stage approximately 3 days after the louse has settled on a host and further increase throughout development accommodating a gradual increase in the number of immune cells [29,30] (Fig. 1), *LsLGP3* KD was induced in nauplii in addition to adult lice, and fish were subsequently infested with copepodids or adult lice. Scaled skin samples were taken from fish infested with copepodids and sampled when lice were at the chalimus I stage 5 and 7 dpi, and from fish infested with adults and left for 21 dpi, and the transcriptomic responses of infested salmon were analysed.

As expected, based on previous publications [19,22], most genes found to be differently expressed were significantly altered at the lice infestation site as compared to both samples taken from untreated fish and non-infested area on infested fish. Only a few genes were found using the stringent method, examining significantly regulated genes between the KD and control group (Supplementary file 2), with 13 identified at 5 dpi (Fig. 2), none at 7 dpi and three underneath adult lice at 21 dpi (p-adjusted <0.05). The transcript levels of genes which were significantly differentially regulated were found to typically encode proteins mainly expressed by immune cells, such as hemopoietic cell kinase, acidic mammalian chitinase, and lysozyme, and were genes that generally displayed a relatively high expression level (Fig. 2). More differently expressed genes between skin infested with KD and control lice were found (p-adjusted <0.05) (Supplementary file 2, Supplementary Fig. 2). There were some transcript with biologically relevant

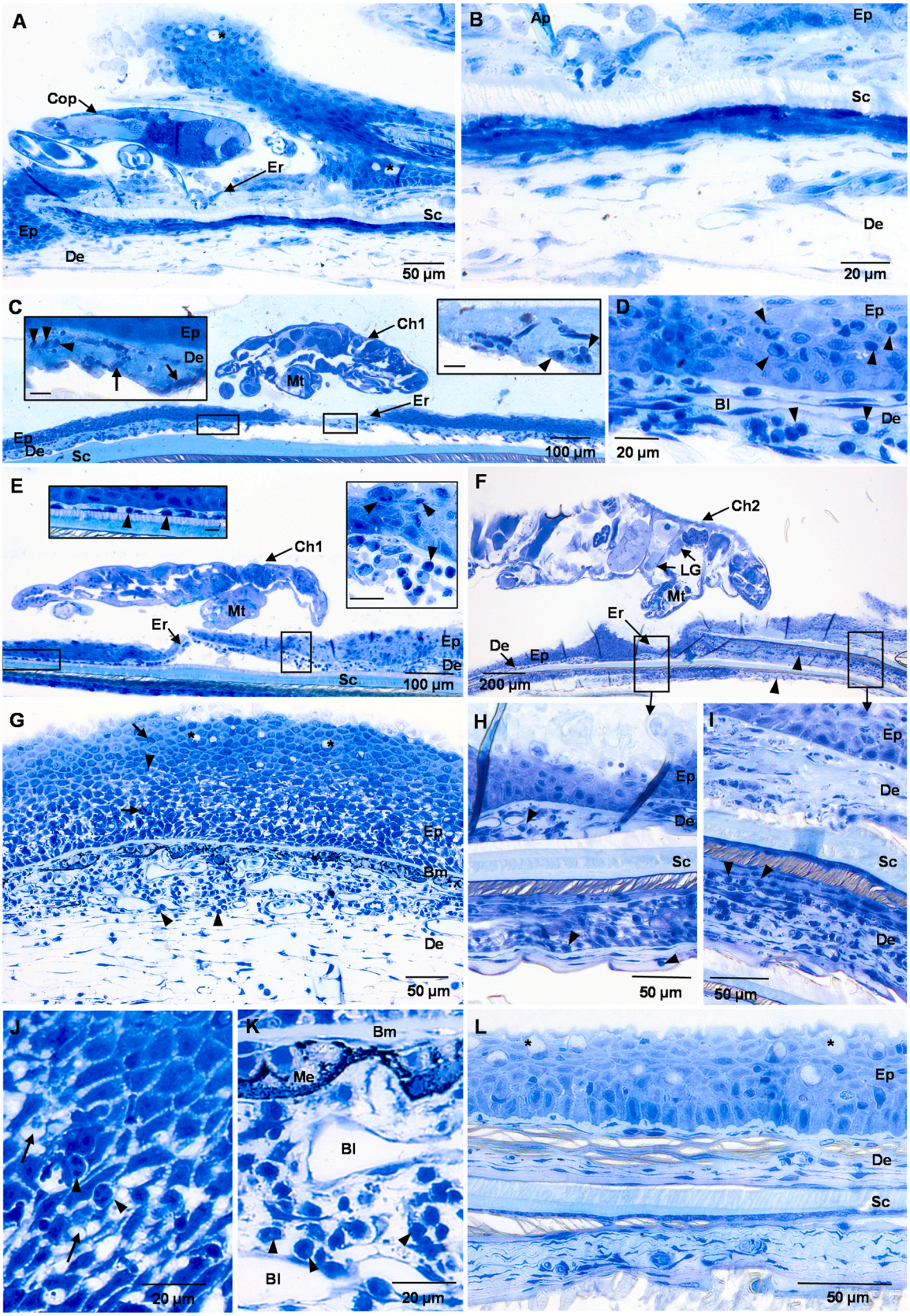

(caption on next page)

Fig. 1. Histopathology in Atlantic salmon scaled skin at the salmon louse attachment site from plastic embedded sections stained with toluidine blue. (A, B) Skin from copepodid (Cop) attachment site (3 dpi) displaying erosion and a lack of immune cell infiltration. (C, D) Chalimus I (Ch1) attachment site (5 dpi). C) Epidermal erosion is seen underneath the lice mouth tube (Mt), with influx of immune cells (examples of immune cells are indicated with arrowheads) in both epidermis and dermis. Close to the lice inflicted lesion, however, fewer immune cells were seen and insert shows higher magnification of these sites (scale bar 10 μm). Here, an area with cell debris was also observed indicated with arrows. (D) From the same specimen showing higher magnification next to the lice, with immune cell infiltration in both epidermis and dermis, where many polymorphonuclear-like cells were seen. (E) Chalimus I (Ch1) attachment site (7 dpi) with skin erosion close to where the lice mouth tube is situated. Immune cells are seen in both dermis and epidermis, with higher number of cells seen anterior to the lice attachment site. Insert shows higher magnification of immune cells (scale bar 10 μm). (F) Chalimus II (Ch2) attachment site (12 dpi) displaying immune cell infiltration extending deeper into the stratum spongiosum. The immune cells are, however, more numerous posterior to the lice, whereas directly underneath the mouth tube only a few immune cells are seen. (H–I) Shows higher magnification of marked area in F, where immune cell influx can be seen in the deeper dermal layers. (G) Adult louse attachment site (51 dpi) displaying keratocyte degeneration of the epidermis close to the basement membrane, while more apical keratocytes show a normal morphology with intact cell junctions. A few melanomacrophages (arrows) and polymorphonuclear-like cells could also be seen in the epidermis, while a more prominent influx of immune cells is seen in the dermis. (J) Higher magnification of epidermis with polymorphonuclear-like cells infiltration, and keratocyte degeneration (indicated by arrows) are seen. (K) Higher magnification of dermis, where many immune cells mainly polymorphonuclear-like cells are seen. (L) Skin of fish infested with chalimus I lice, 7 dpi, at unaffected areas. There are no visible granulocyte or macrophage infiltration in either epidermis or dermis. All abbreviations: Ep - epidermis, De - dermis, Sc – scale, Bm – basement membrane, Er – erosion, Cop – copepodid, Ch1 – Chalimus I, ChII – Chalimus II, Mx – maxilliped, Mt – mouth tube, LG – labial gland, Bl – blood vessel, Me – melanocytes, * - mucus cells, arrowhead – immune cells.

expression patterns, including transcript encoding *tumour necrosis factor α receptor, sialoadhesin* and *mucin-2-like*. Three paralogues of the gene nucleotide-binding oligomerization domain (NOD)-like receptor (NLR) family were significantly upregulated in fish infested with KD lice, especially away from the lice infestation site (Fig. 2, Supplementary Fig. 2). The *LsLGP3* transcript level in LsLGP3 KD lice was reduced by 98 %, with a decrease of 6 Ct-values from 21 to 27 (Supplementary Fig. 3). No difference in lice count on the fish in KD compared to the control lice was observed in between any of the sample groups or time points (Supplementary Fig. 3).

3.4. LsLGP3 decreases the viability of Atlantic salmon leukocytes

As immune related transcript levels increased under LsLGP3-KD lice and B- and T-cell marker transcripts and total RNA-yield was found to decrease in primary head kidney leucocytes after recLGP3 exposure [30], we hypothesised that LsLGP3 either is inhibiting immune cell attraction or is inducing cell death. Therefore, the viability was measured in PBLs from Atlantic salmon treated with recLGP3 *in vitro*. A decreased viability of leukocytes in a concentration dependent manner was seen, where the solution was cloudy and the viability was decreased by around 30 and 40 percent, respectively, for the two highest concentrations after a 6-h exposure to recLGP3 (Fig. 3A). Moreover, most nucleic acids in leukocytes were stained with the cell death marker propidium iodide, and the cell morphology were found to be significantly disrupted in ColorRapid stained cells after a 2-h LsLGP3 exposure (100 μg) (Fig. 3B), further indicating that LsLGP3 is inducing cell death in Atlantic salmon immune cells. Longer incubation times did not induce further decrease in live cells (results not shown).

Enriched populations of monocytes, granulocytes, IgM^+ B-cells and NCC/T-cells were further exposed to recLGP3 to investigate whether cell death was induced in specific cell types. Monocytes were obtained by collecting adherent cells, B-cells by using anti-IgM antibody and FACS, while T-cells and granulocytes were separated based on size and granularity in FACS (Fig. 4A). The cellular properties were determined by stained cytospin preparations (MPO, ColorRapid), which showed high purity and homogenous cell populations in the granulocyte and IgM^+ B-cells fraction (Fig. 4B, C, F, G), while the monocyte fraction and NCC/T-cell fraction was more mixed (Fig. 4D, E, H, I).

Each enriched cell population was then exposed to recLGP3 for 6 h, and the viability was measured using CASY. All cell populations displayed a significant decrease in viability compared to the non-exposed control cells, while no significant difference was detected between the different cell populations (Fig. 5A). To further investigate the mechanism inducing cell death, the morphology of the cells was observed after 1 h of recLGP3 exposure using SEM (Fig. 5B–D, E, G, H, J, K, M, N). Most cells in all four populations formed membrane protrusions with a "beads on a string" like morphology (Fig. 5B, Supplementary Fig. 4), with similar looking debris observed in all populations (Supplementary Fig. 4E). Especially in the IgM^+ B-cell and monocyte enriched population, cell aggregations with large amounts of debris were observed (Fig. 5E–K). The protrusions seemed to extend from one focus and be covered by cell membrane. Nevertheless, we further wanted to confirm that these protrusions were not chromatin neutrophil extracellular traps (NETs) formation, by analysing the uptake of SYTOX-Green by extracellular DNA and the level of intracellular calcium (Supplementary Fig. 5). No evidence of extracellular chromatin content in the string-like structures were found.

3.5. LsLGP3 function is more effective on salmonid leukocytes

As LsLGP3 is secreted at the salmon louse feeding site, LsLGP3 may also interact with red blood cells (RBCs) and skin. Therefore, the viability and/or cell morphology of epidermal cells in skin and RBCs exposed to recLGP3 were examined. Morphological changes were seen neither in RBCs or epidermal cells having intact micro ridges and tight junctions (Fig. 6A), and accordingly, viability of RBCs remained unchanged after recLGP3 exposure (Fig. 6B). Furthermore, the viability of leukocytes from four additional fish species were analysed after recLGP3 exposure, including the salmon louse resistant pink and coho salmon and the two non-hosts Atlantic cod and lumpfish. However, recLGP3 treated leukocytes from Atlantic cod and lumpfish displayed only a minor decrease in viability, yet significantly different form the non-exposed control and exposed leukocytes from Atlantic salmon (Fig. 6C). Viability of pink and coho salmon leukocytes after recLGP3 exposure also decreased to a similar degree to that of Atlantic salmon leucocytes (Fig. 6C and D). The cell morphology of coho leukocytes exposed to recLGP3 showed small holes, swelling and some membrane protrusions (Supplementary Fig. 6).

3.6. Positively charged amino acids are important for LsLGP3 function

The specificity of the recLGP3 towards certain cell types and fish species suggest that LsLGP3 binds specifically to a distinct ligand. To depict which amino acids that are important for this binding, two distinct regions with positively charged amino acids in the protein sequence were targeted, predicted to be in an outer loop of the protein structure. At these two sites three (A) and two (B) amino acids were substituted from positively charged to negatively charged amino acids (Fig. 7A), resulting in the formation of the recombinant proteins AΔLsLGP3, BΔLsLGP3 and ABΔLsLGP3. The effect of these amino acid substitutions on the proteins ability to decrease the viability of Atlantic salmon leukocytes were investigated. Amino acids substitution at only one site (AΔLGP3, BΔLGP3) caused a significant decrease in cell viability compared to the negative control like the wild-type protein (Fig. 7B). However, substituting all five amino acids in ABΔLsLGP3

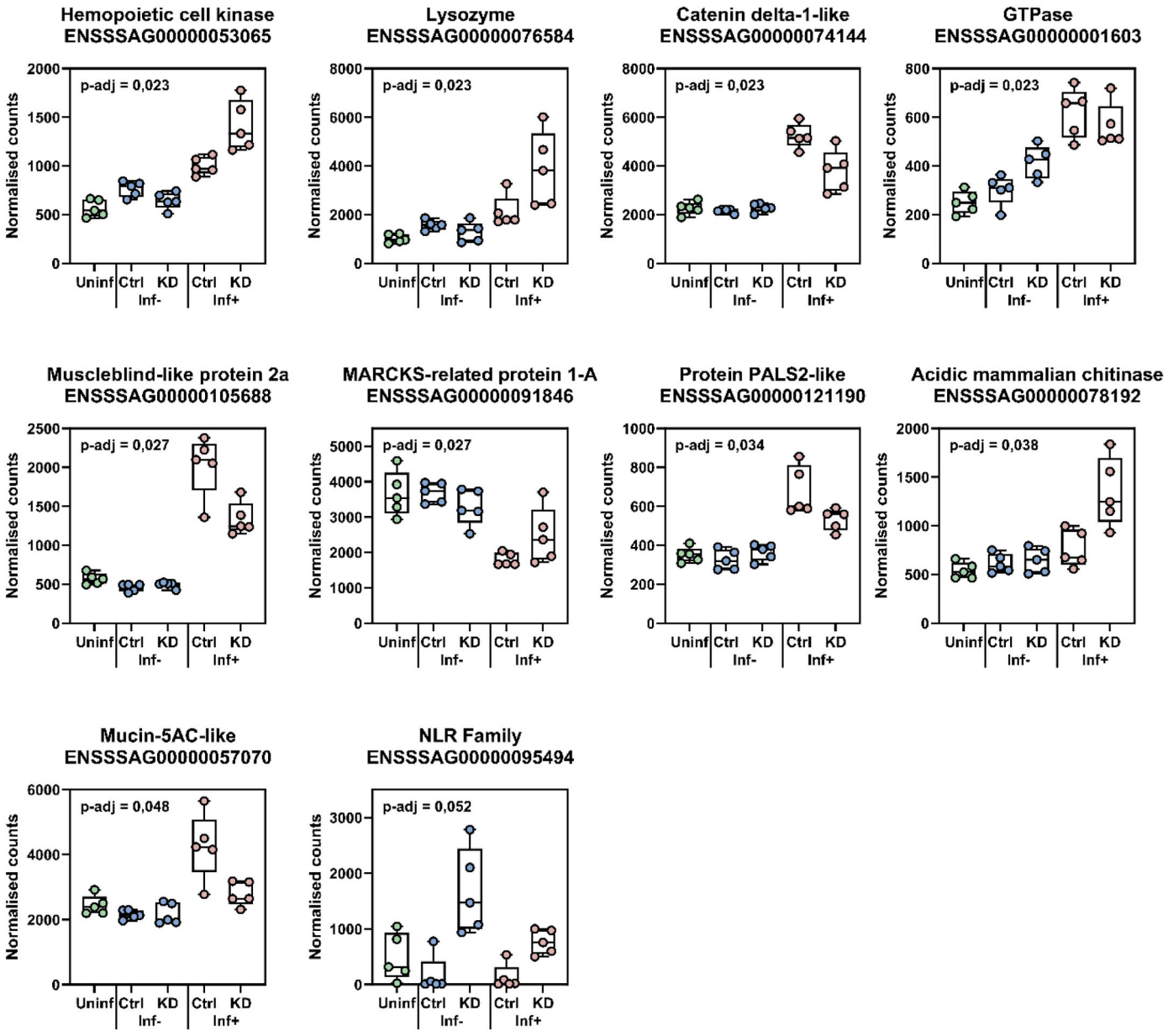

Fig. 2. RNA-sequencing of Atlantic salmon skin during infestation with LsLGP3 knock-down salmon louse. mRNA transcript levels of selected significantly differentially regulated genes analysed by RNA-sequencing of scaled Atlantic salmon skin samples taken at and away from the LsLGP3 knock down (KD) and control (Ctrl) salmon louse infestation site. Normalised counts for each sample are plotted above a boxplot of median ± interquartile range (n = 5) in uninfested fish (Uninf, green dots), and infested fish at the lice attachment site (Inf+, red dots) and non-attachment site (Inf-, blue dots) for Ctrl and *LsLGP3* KD salmon lice. The calculated p-adjusted values are indicated in the upper left corner. The p-adjusted value indicates the significance after testing the group-specific effect of the lice treatment, while controlling for individual effects, calculated by DeSeq2's Wald tests, adjusting for multiple tests using DeSeq2's Benjamini-Hochberg correction. The genes are sorted by p-adjusted value.

abolished the protein's ability to induce cell death.

4. Discussion

LsLGP3 has previously been suggested to have an immune modulatory function suppressing cellular immune responses [30]. Dampening of cellular responses is likely to be of high importance for the salmon louse, as to establish and survive on its host and reproduce. The present study advances the understanding of LsLGP3's function through novel *in vivo* and *in vitro* investigations to elucidate this mechanism, where LsLGP3 can be suggested to directly induce cell death in immune cells. It was also ascertained that LsLGP3 protein was in fact expressed by the labial gland and may be secreted on to the host skin. The implication here is that LsLGP3 may interact with host proteins on the surface of cutaneous immune cells and have an important role in the host-parasite interaction by eliminating these cells.

Building on these findings, conducting *in vivo LsLGP3*-KD with subsequent infestation studies to analyse the local immune response at the lice feeding site, represents a way to analyse the function of LsLGP3 without knowing the physiological concentration of the protein or size. Though, a knock down is not a knockout, and LsLGP3 will still be secreted by *LsLGP3*-KD lice, though likely with a significantly reduced concentration as the mRNA level in KD lice was reduced by 98 %, corresponding to a decrease of 6 on the Ct-value scale. However, *LsLGP3* is a highly expressed gene and will probably still be present in the saliva secretions of *LsLGP3*-KD lice. Nevertheless, the transcriptomic analysis

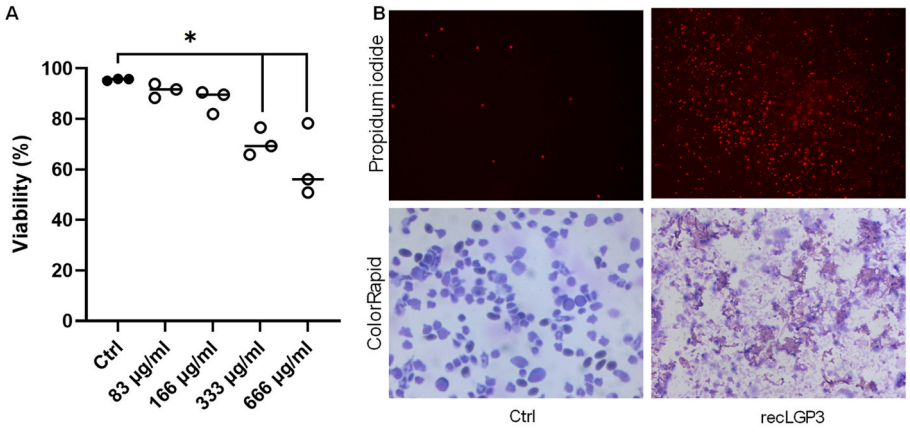

Fig. 3. Viability analysis of PBLs exposed to recLGP3. (A) Cell viability measurements of 5 *10^5 Atlantic salmon leukocytes after either 83, 166, 333 or 666 µg/ml recLGP3 exposure for 6 h. N = 3. Significant differences ($p < 0.05$) from the control are indicated by asterisks (*). (B) Intracellular DNA staining (propidium iodide) and ColorRapid staining of Atlantic salmon leukocytes after 112 µg recLGP3 exposure for 2 h.

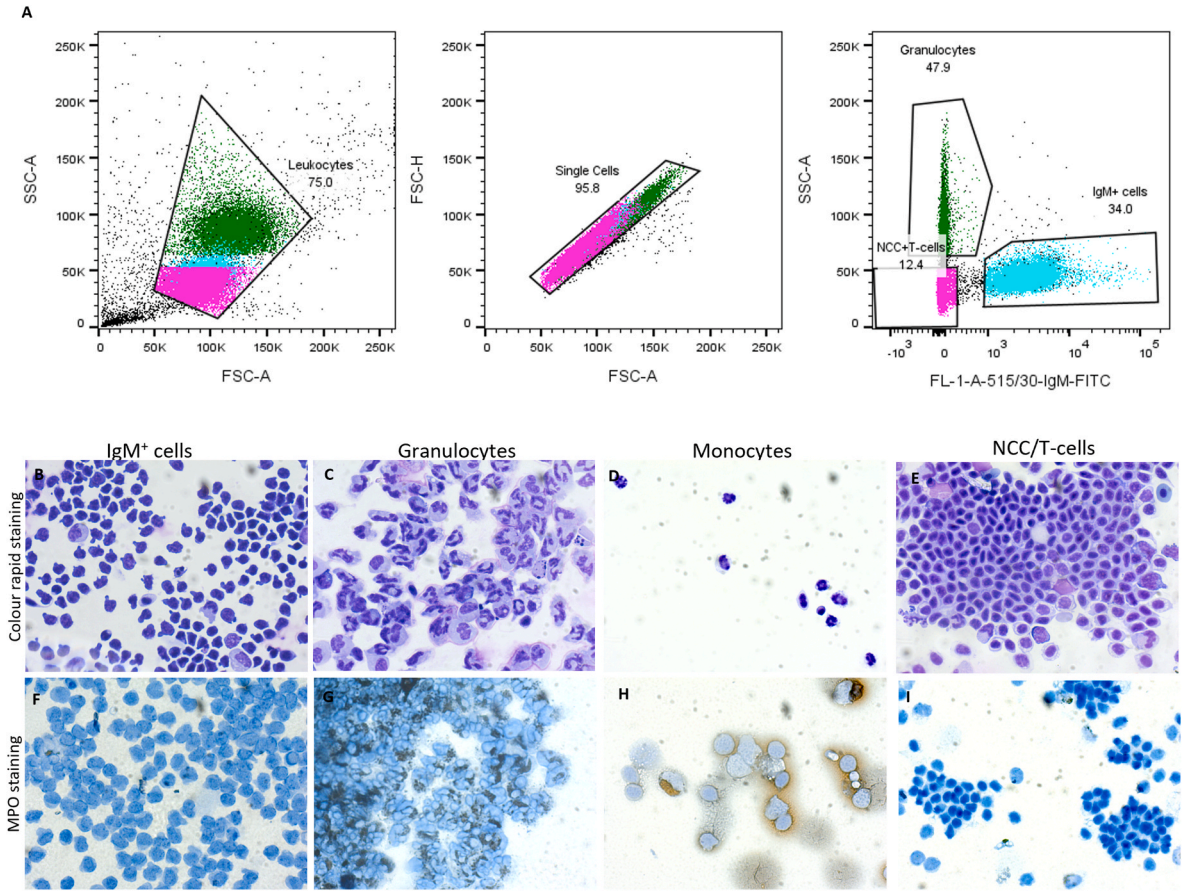

Fig. 4. Sorting of PBLs. (A) FACS gating strategy to obtain enriched populations of Atlantic salmon IgM^+ cell, NCC/T-cells and Granulocytes. Morphological and cytochemical analysis of PBLs; Cytospin preparation of enriched populations of (B, F) IgM + cells, (C, G) Granulocytes, (D, H) Monocytes and (E, I) NCC/T-cells stained with (B–E) ColorRapid and (F–I) Myeloperoxidase (MPO) activity appears as black/brown colouring in the cells.

identified immune related genes which were increased underneath *LsLGP3*-KD lice, such as the most significantly regulated genes encoding for hemopoietic cell kinase (*hck*), lysozyme (*lysc2*), and acidic mammalian chitinase. *Hck* transcripts are suggested to be expressed in myeloid and lymphocyte lineages, to enhance pro-inflammatory cytokine secretions from myeloid cells, promotes macrophage polarisation towards wound healing and enhances immune and epithelial cell invasion [47]. Transcripts for *lysc2* are present in several tissue types such as head kidney, spleen, liver, gills and to some extent in skin, and especially expressed by Atlantic salmon granulocytes and macrophages [48,49]. Lysozymes function as anti-bacterial enzymes by hydrolysis of peptidoglycan in the cell wall, especially at mucosal sites [50], and have also been suggested to have an immunomodulatory role by enhancing bacterial product release, activating pattern recognition receptors in the host [51]. Also *acidic mammalian chitinase* is expressed in innate immune cells but also epithelial cells, which may be induced by IL4/13A [52].

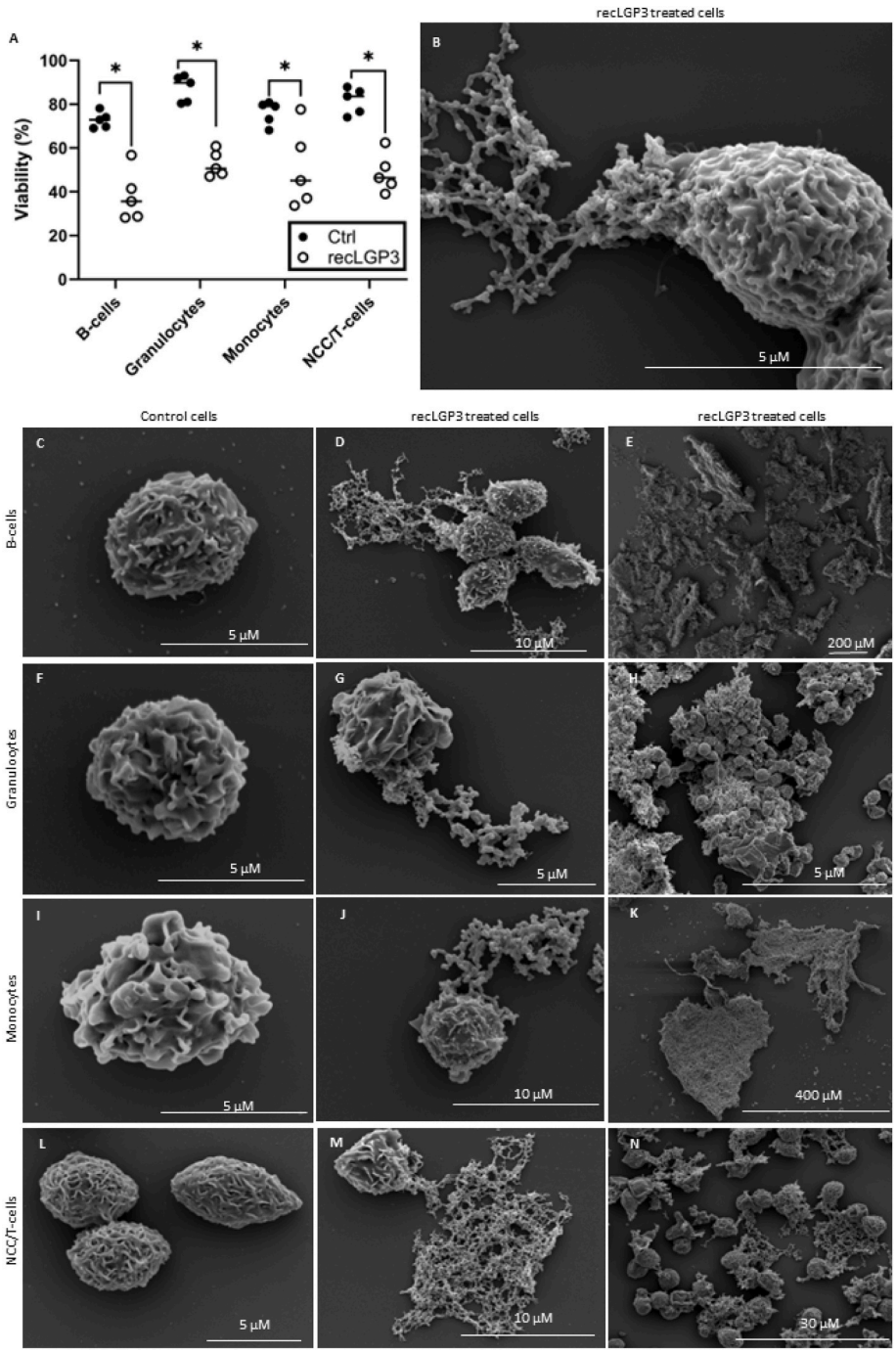

Fig. 5. Analysis of enriched populations of peripheral blood leukocytes exposed to recLGP3. (A) Viability measurement of enriched populations of 5 *10^5 Atlantic salmon B-cells, granulocytes, monocytes and NCC/T-cells exposed to 112 µg (373 µg/ml) recLGP3 for 6 h measured by CASY TT, n = 5. Significant differences ($p < 0.05$, *t*-test) between control and LsLGP3 exposed cells are marked with asterisks (*). Fixed cells captured with Scanning Electron Microscopy (SEM) of (B) leukocytes exposed to 112 µg(373 µg/ml) recLGP3, and enriched populations of (C–E) IgM + cells, (F–H) Granulocytes, (I–K) Monocytes and (L–N) NCC/T-cells, with (C, F, I, L) negative control and (D, E, G, H, J, K, M, N) recLGP3 exposed cells, with high and low magnifications, n = 5.

The exact mechanism of acidic mammalian chitinase still remains elusive, but is suggested to indirectly increase CCL2, CCL17 and CXCL secretion [53], causing an inflammatory cell infiltration by increasing macrophage and T-cells recruitment, thereby regulating a Th_2 mediated response [54]. Interestingly, *acidic mammalian chitinase* was significantly up-regulated in head kidney in louse infested pink salmon [25], and in skin in juvenile pink salmon after immunity maturation and louse resistance has been gained [55], indicating that *acidic mammalian chitinase* may be an important immune regulator in salmon louse clearance. Also interesting is the significant increase in the systemic expression of three transcripts encoding for the NLR-family in fish infested with *LsLGP3* KD lice. A systemic skin and head kidney response to louse has also been seen in previous studies, with an increase in *il4/13a* transcripts [19,22]. However, there was a notable decrease in expression underneath the LsLGP3 KD lice compared to non-attachment site in the same fish. Despite this, expression levels were still significantly different compared to fish infested with control lice. The NLR-family proteins are pattern-recognition receptor involved in regulation of innate immune responses, and are found in immune and epithelial cells [56]. Although this observation is based on three paralogues genes, it suggests that

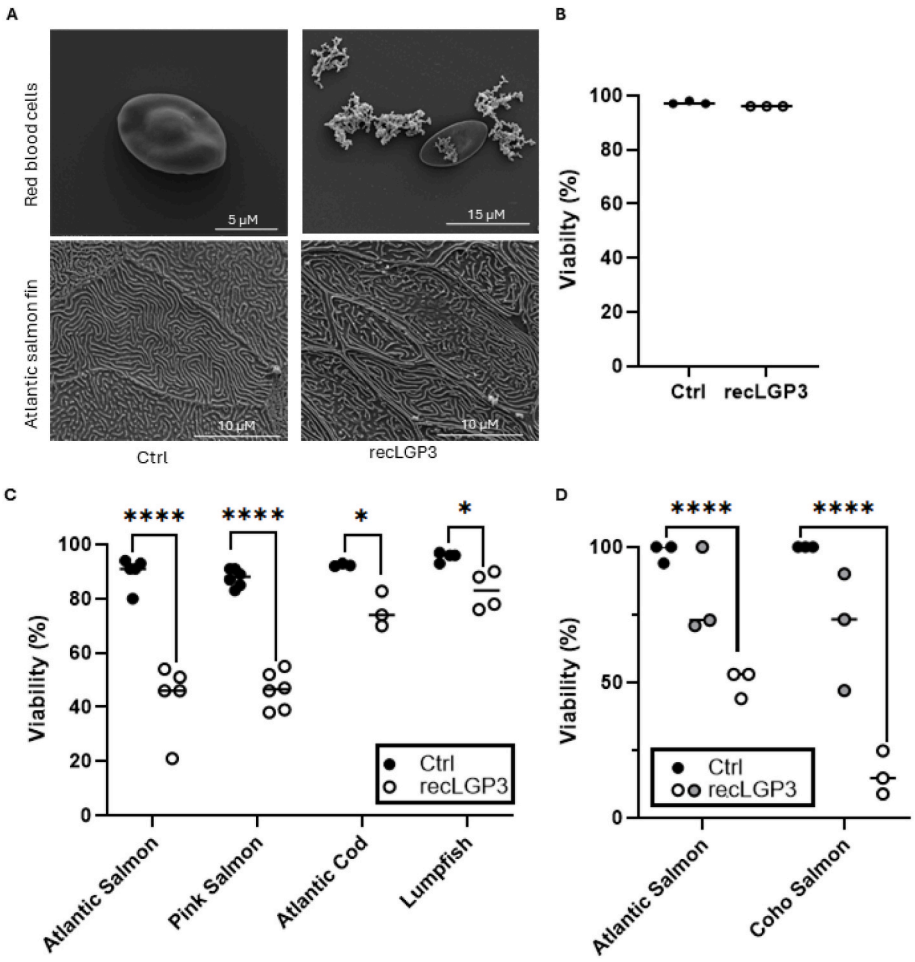

Fig. 6. Tissue, cell type and species comparison after recLGP3 exposure. (A) Scanning electron microscopy of Atlantic salmon blood cells and fins exposed to 112 µg recLGP3 for 1 or 6 h, respectively. (B) Viability of 5 $*10^5$ red blood cells from Atlantic salmon exposed to 112 µg (373 µg/ml) recLGP3 for 6 h, n = 3. (C) Viability of 1 $*10^5$ leukocytes from Atlantic salmon, pink salmon, Atlantic cod and lumpfish exposed to 112 µg (373 µg/ml) recLGP3 for 6 h n = 3–5. (D) Viability 2.5 $*10^5$ of leukocytes from Atlantic salmon and coho salmon exposed to 56 µg (373 µg/ml) and 112 µg(746 µg/ml) recLGP3 showed in grey and white dots, respectively, n = 3. *P < 0.05 ****P < 0.0001.

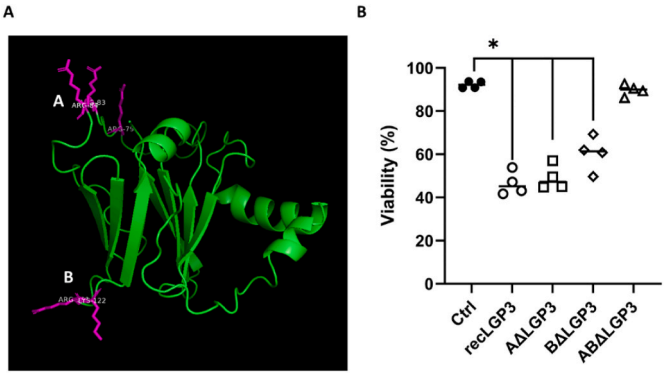

Fig. 7. LsLGP3 structural analysis. (A) Predicted AlphaFold protein structure without signal peptide and indicated substituted amino acids in magenta A: R79E; R83E; R84E, B: R121E; K122E. (B) Atlantic salmon leukocyte viability after 6 h exposure with 112 µg(373 µg/ml) of recLGP3 or the amino acid substituted recLGP3; AΔLGP3, BΔLGP3 and ABΔLGP3 measured using CASY TT, *P < 0.05 n = 4.

LsLGP3 may be involved in dampening a systemic response. An upregulation of transcripts predicted to encode *tnfα-receptor superfamily 14 (tnfrsf14)* was found in fish infested with *LsLGP3* KD lice. TNFRSF14 is proposed to be mainly expressed by immune cells. However, functional studies of *tnfrsf14* in teleost fish have not been conducted, so whether it functions as a death-receptor remains unknown.

Nevertheless, the effect *LsLGP3*-KD lice had on the fish was not found to be prominent but indicates that LsLGP3 has a superficial and localised effect at the site of secretion, namely in lesions close to the mouth tube. The increase in immune cell markers at the infestation site of *LsLGP3*-KD compared to control louse were found to be mainly markers expressed solely by innate immune cells, but this was only detected at the time point where immune cells started to appear at the infestation site, at 5 dpi. Later, the immune cell influx was more prominent both anterior and laterally to the lice inflicted wounds, and if the effect of LsLGP3 is limited to the lesions inflicted by localised epidermal feeding, higher abundance of dermal immune cells could have diluted the localised effect of *LsLGP3*-KD to undetectable levels. Supporting this is the notion that fewer immune cells were seen in the dermis close to the mouth tube of chalimus lice at all sampled time points. And even though the histological analysis were not executed on the same individuals as those from which the transcriptional data were obtained from, this still indicates the status of the control fish in the transcriptomic study since findings in the present study are supported by previous histological findings in Atlantic salmon and other susceptible salmonid species as rainbow trout and chinook salmon [3,4,19,27]. Evidently, an influx of mainly polymorphonuclear-like cells were not only seen in the dermis, but also in the epidermis, further pinpointing the importance of LsLGP3 in the

host parasite interaction as these immune cells will be closer to the lice and thus have a greater potential for affecting the lice. Interestingly, when *LsLGP3* transcripts peak at the adult stage, immune cells localised to the epidermis were almost absent. This may indicate that LsLGP3 could induce cell death in epidermal localised immune cells close to the attachment site, thereby lowering immune cell numbers in the epidermis. Furthermore, the downregulation of mRNA transcript levels of B and T-cell markers such as *igm, igt, igd, tcrα, cd8α, cd4* and cytokines and immune cell markers such as *il1β, il4/13a, gata3* and *mhc2* at the adult infestation site further supports this hypothesis [22]. Particularly naïve T-cells are to be found in the skin, and the transcriptomic data suggest that T-cell maturation does not occur [22,57,58]. However, the epidermal changes were much more evident close to the dermis where a more prominent immune cell numbers were seen, indicating that the changes are inflicted by the immune response and maybe not the lice. Though, it should be mentioned that the epidermis was more intact underneath adult lice as compared to copepodid and chalimus lice, likely as the lice now mainly feeds of the host blood and therefore only induces minor damage to the epidermis around the mouth tube on their way down to the dermal blood supply (Supplementary Fig. 1) [4,19,20]. This study has shown the histological effects of the salmon louse itself on Atlantic salmon under controlled laboratory conditions, and the extensive lesions seen underneath adult lice in the field are most likely due to secondary infections in the wound and/or very high parasitic loads [4,5,59,60]. Therefore, these processes are likely to be complex, influenced both by louse and host responses, but also environmental factors. What can be noted is, however, that immune cells become more evident at the attachment site as the infestation progresses, correlating with the increased expression of *LsLGP3* during salmon louse development.

Even though the *in vivo* studies indicated that LsLGP3 decreases the number of immune cells at the site of infestation, further *in vitro* studies were necessary as to confirm this, and to analyse the specific cell death mechanism. As quantifying the amount of LsLGP3 secreted onto the fish remains a challenge, the concentration that each immune cell is subjected to *in vivo* is difficult to replicate in *in vitro* experiments. This because the concentration of LsLGP3 secretions is unknown, and so is the feeding-frequency of salmon louse or whether the labial gland secretions are deposited onto the skin also in between feeding. We have observed that the louse probably ingests intermittently, and the anatomical positioning of the labial gland ducts adjacent to the mandible teeth and strigils used for feeding [32], imply that secretion of labial gland proteins correlates with feeding. Moreover, mobile louse seem to aggregate together at certain regions of the skin [61,62], thereby a more continuous effect and a higher concentration of LsLGP3 is expected at the infestation site of multiple lice. Despite, the inability to ascertain a physiological concentration, the recLGP3 concentration that resulted in a 40–50 % decrease in leukocyte viability in *in vitro* experiments was used in the present study.

Several complementary methods were used to determine cell viability and concluded with similar results. First, cell viability was quantified using a CASY cell counter, which quantifies the percentage of viable cells and cellular debris (Casy Counter). The viability is quantified by electrical current exclusion by loss in resistance from the cytoplasmic membrane in dead cells, instead the nucleus in non-viable leukocytes with a diameter less than 6 μM is measured. After 6 h of recLGP3 exposure, a viability of 40–50 % was measured. Moreover, SEM analysis insinuated a more prominent decline in cellular integrity within 1–2 h after recLGP3 exposure. Concurrently, an increased prevalence of PI positively stained cells after recLGP3 exposure implies that true death rates after recLGP3 exposure may by higher than that indicated by the CASY analyses. CASY analyses were still used due to the objective quantification of cells. Altogether, this clearly indicates a reduction in peripheral blood leukocyte viability by recLGP3. Leukocytes were then sorted to obtain enriched cell populations, as to analyse whether recLGP3 exposure induces cell death in all immune cell types. The purity of the populations was, however, variable. The IgM^+-cells were all MPO negative and showed lymphocyte morphology and size, which indicates high purity of B-cells. The granulocyte population were positive for MPO and mostly contained polymorphonuclear cells. The monocyte population had some MPO positive cells and many cells with monocyte morphology, but also cells with a more polymorph nucleus. The absence of commercially available antibodies specific to T-cell markers resulted in a T-cell fraction of reduced purity, though most cells displayed lymphocyte morphology. Cytospin preparation revealed a diversity in cell morphology, predominantly lymphocyte like and some NCC and monocytes. Despite the cell variation, no statistically significant difference was noted across the different cellular populations, and overall, recLGP3 seemed to affect all types of immune cells. However, given the limitations, definitive conclusions regarding effect of recLGP3 exposure on T-cells, remains elusive. Notably, no detectable decrease in viability was observed in salmonid epidermal cells or red blood cells after recLGP3 exposure. This resilience may be advantageous for the parasitic louse, which relies on the blood and skin for nutrition, necessitating the preservation of intact red blood cells and precluding any excessive damage to host epidermal cells. More importantly, these findings imply that the mechanism of recLGP3 is specific to leukocytes.

The morphology of the recLGP3-exposed leucocytes suggested that LsLGP3 might trigger an apoptosis pathway, resulting in the formation of apoptotic bodies seen as long cell-membrane covered blebbed protrusions. This is supported by the downregulation of *ifng* and the lack of *il1β* induction previously seen in recLGP3 exposed leukocytes, indicating there is no additional attraction of immune cells through caspase-8 dependent IL-1β release [30,63]. Apoptosis is programmed cell-death which often is immunogenically silent or anti-inflammatory, where little intracellular components are released into the tissue, and macrophages are recruited and engulf apoptotic cells by efferocytosis [64]. In contrast, necrosis is often a pro-inflammatory process due to the release of intracellular damage-associated molecular patterns. Apoptosis is more controlled and morphological changes occurs in three steps: plasma membrane blebbing, formation of apoptotic membrane protrusions and generation of membrane-bound extracellular vesicles, apoptotic bodies [65–68]. Membrane protrusions can have variable morphology depending on the cell type, such as strings or "beads-on-a-string" structures [65,67]. The membrane protrusions were often observed to be connected between the cells, and some had varied morphology, and the "beads-on-a-string"-like structures were also seen released from the cells (Supplementary Fig. 4). Similar membrane protrusions followed by apoptotic bodies formation with beaded string-like structures have also been observed in UV-treated human leucocytes [65,67,69,70]. We therefore tried to induce this in Atlantic salmon leucocytes by UV-light treatment for 2 h, however, only cell swelling was seen after UV-treatment (Supplementary Fig. 4), and no apoptotic "beads-on-a-string" as seen in human monocytes. We therefore wanted to analyse if these recLGP3-induced membrane protrusions may be a result of chromatin neutrophil extracellular traps (NETs) formation and subsequent NETosis. NETs are chromatin structures released from neutrophils with bactericidal activity by histones, neutrophil elastase and MPO [71–73]. NET release may be followed by the cell death mechanism NETosis [74]. However, this hypothesis was rejected upon the absence of SYTOX-Green positive extracellular DNA fragments, coupled with no increase in intracellular calcium levels (Supplementary Fig. 5), as has been seen upon NETosis in both Atlantic salmon and mammals [75,76]. Notably, the recLGP3-induced membrane protrusions were observed in all enriched cell populations, with a pronounced preponderance in IgM^+ cells, further suggesting that they are not due to neutrophil trap formation. Moreover, trap formation is a rather unspecific process [77], and further LsLGP3 mutational analysis suggested that LsLGP3 specifically bind to e.g. a cell surface receptor to induce apoptosis. The synthesis of an inactive recLGP3, designated ABΔLGP3, implicates the crucial role of charged residues, specifically arginine and lysine amino acids, in the binding efficacy of the protein to its ligand. The mutant could, however, have an incorrect folding that would further inhibit its

ligand binding capability. Though, given that the protein had high solubility even at high concentrations (10 mg/mL), it is unlikely that the amino acid substitutions have drastically altered the conformation. Therefore, ABΔLGP3 functions as a negative control in the experiment, confirming that the observed decrease in leukocyte viability following recLGP3 exposure is due to a targeted biological reaction rather than non-specific effects as NET formation towards e.g. residual contaminants from the protein purification. Additionally, leukocytes from Atlantic cod and lumpfish displayed only a modest decrease in viability following recLGP3 exposure, as compared to Atlantic salmon leukocytes, which further supports a specific mode of action. The analogous lack of response manifested by both lumpfish and Atlantic cod leukocytes further suggests that recLGP3 has an affinity for or is adapted to bind specifically to membrane receptors on salmonid leukocytes.

As the pink salmon is highly resistant to salmon louse, it was somehow surprising that recLGP3 mediated a decreased viability of pink salmon leukocytes at similar levels as that seen in Atlantic salmon leukocytes exposed to recLGP3. Though, the differential susceptibility observed in pink salmon seems to stem from their ability to eliminate lice during the copepodid stage [24], whereas *LsLGP3* mRNA transcript are not present until 2–3 days post infestation and increases during lice development when on Atlantic salmon [29,30]. Interestingly, LsLGP3 is one of only two labial gland genes that are expressed as a response to host settlement and was also found to be induced in lice infesting pink salmon [29]. Thus, immune cell responses do not seem to be part of the pink salmon resistance mechanism. Interestingly, *LsLGP3* mRNA transcripts are detected in lice sampled together with coho salmon fin tissue 2 to 14 dpi, yet, the mRNA transcript level of *LsLGP3* in the louse does not increase throughout the infestation as seen in lice on Atlantic and Pink salmon, when normalised against the *elongation factor 1a* reference gene, and compared to other labial gland genes who seems to increase during the infestation [28,29]. Even though this may be due to low total lice counts in the sample or that the lice mRNA was degraded in the sample, it indicates that LsLGP3 expression is not at an optimal level in lice infesting coho salmon. This study also indicates that coho salmon leukocytes are affected by recLGP3 exposure similar to Atlantic salmon (Fig. 6, Supplementary Fig. 6). The cell morphology differed between the two species when exposed to recLGP3 and whether the mechanism of cell death is similar or not cannot be determined in this study. This may indicate that coho leukocytes may not encounter high levels of LsLGP3, which allows for an influx of immune cells to the louse infestation site [27,28].

5. Conclusion

LsLGP3 has been found to specifically decrease the viability of salmonid leukocytes, probably by inducing apoptosis. As opposed to necrosis that would induce inflammatory responses, apoptotic cells do not necessarily induce such responses if they are phagocytosed prior to the release of intracellular content and can even be anti-inflammatory [78]. Thus, inducing immune cell apoptosis offers an effective mechanism for immune dampening. This study has therefore laid the foundation for innovative and sustainable strategies for maintaining low lice numbers in salmon farms. These strategies could include the development of vaccines or the use of gene editing to produce salmon resistant to salmon louse. LsLGP3 shows potential as a vaccine antigen that could aid in lice rejection. Furthermore, it is crucial to identify the binding receptor for LsLGP3 on salmon, as this can contribute to producing salmon resistant to salmon lice. Modifying this binding receptor could contribute to an increased influx of immune cells to the infestation site and thereby enhance lice rejection. When these strategies are combined with sterile salmon, it could significantly improve aquaculture sustainability and fish welfare.

CRediT authorship contribution statement

Helena Marie Doherty Midtbø: Investigation, Formal analysis, Validation, Visualization, Writing – original draft. **Andreas Borchel:** Investigation, Formal analysis, Writing – review & editing. **H. Craig Morton:** Formal analysis, Writing – review & editing. **Richard Paley:** Investigation, Writing – review & editing. **Sean Monaghan:** Investigation, Formal analysis, Writing – review & editing. **Gyri Teien Haugland:** Conceptualization, Investigation, Formal analysis, Writing – review & editing. **Aina-Cathrine Øvergård:** Conceptualization, Investigation, Formal analysis, Project administration, Writing – review & editing.

Declaration of interest

None.

Disclosure

During the preparation of this work the first author used Microsoft Copilot to improve the readability and language. After using this tool, the authors reviewed and edited the content as needed and take full responsibility for the content of the publication.

Funding

This work was funded by the Norwegian Seafood Research Fund (FHF) project ModuLus, grant number 901564 and CrispResist, grant number 901631. The Genomics Core Facility (GCF) at the University of Bergen, which is a part of the NorSeq consortium, provided services on RNA-sequencing; GCF is supported in part by major grants from the Research Council of Norway (grant no. 245979/F50) and Bergen Research Foundation (BFS) (grant no. BFS2017TMT04 and BFS2017TMT08).

Acknowledgements

The authors are very grateful to the following people at the Department of Biological Sciences, University of Bergen; Frank Nilsen for kindly donating pink salmon, Heidi Kongshaug for performing experiments on coho salmon, Lindsey Jane Moore and Patrick Alexander Nelsson for laying percoll density gradients, Per Gunnar Espedal for fish maintenance and providing salmon louse, and Pavinee Nimmongkol for preparation of specimens for SEM and histology. We thank Irene Heggstad at the Laboratory for Electron Microscopy, University of Bergen for providing expertise on SEM. We are grateful to Brith Bergum at the Flow Cytometry Core Facility, Department of Clinical Science, University of Bergen for providing expertise and performing cell sorting. The authors thank Mark D. Fast at the University of Prince Edward Island and Cindy Edris from the Quinsam Hatcher, Fisheries and Oceans in Canda for coordinating the delivery of coho eggs and providing husbandry advice.

Appendix A. Supplementary data

Supplementary data to this article can be found online at https://doi.org/10.1016/j.fsi.2024.109992.

Data availability

The data is made available on PRJNA1089937 and in supplementary files, and in Bio Project number: PRJNA1089937

References

[1] P. Brandal, E. Egidius, I. Romslo, Host blood: A major food component for the parasitic copepod Lepeophtheirus salmonis Kroeyeri, vol. 1838, 1976 crustacea: caligidae.

[2] R. Wootten, J.W. Smith, E.A. Needham, Aspects of the biology of the parasitic copepods *Lepeophtheirus salmonis* and *Caligus elongatus* on farmed salmonids, and their treatment, Proc. R. Soc. Edinb. Sect. B Biol. Sci. 81 (1982) 185–197, https://doi.org/10.1017/S0269727000003389.

[3] M.W. Jones, C. Sommerville, J. Bron, The histopathology associated with the juvenile stages of *Lepeophtheirus salmonis* on the Atlantic salmon, *Salmo salar* L, J. Fish. Dis. 13 (1990) 303–310, https://doi.org/10.1111/j.1365-2761.1990.tb00786.x.

[4] H. Jònsdottir, J.E. Bron, R. Wootten, J.F. Turnbull, The histopathology associated with the pre-adult and adult stages of *Lepeophtheirus salmonis* on the Atlantic salmon, *Salmo salar* L, J. Fish. Dis. 15 (1992) 521–527, https://doi.org/10.1111/j.1365-2761.1992.tb00684.x.

[5] A. Grimnes, P.J. Jakobsen, The physiological effects of salmon lice infection on post-smolt of Atlantic salmon, J. Fish. Biol. 48 (1996) 1179–1194, https://doi.org/10.1111/j.1095-8649.1996.tb01813.x.

[6] S.E. Barker, I.R. Bricknell, J. Covello, S. Purcell, M.D. Fast, W. Wolters, D. A. Bouchard, Sea lice, *Lepeophtheirus salmonis* (Krøyer 1837), infected Atlantic salmon (*Salmo salar* L.) are more susceptible to infectious salmon anemia virus, PLoS One 14 (2019) e0209178.

[7] B. Finstad, P.A. Bjørn, A. Grimnes, N.A. Hvidsten, Laboratory and field investigations of salmon lice [*Lepeophtheirus salmonis* (Krøyer)] infestation on Atlantic salmon (*Salmo salar* L.) post-smolts, Aquacult. Res. 31 (2000) 795–803, https://doi.org/10.1046/j.1365-2109.2000.00511.x.

[8] L. Tort, Stress and immune modulation in fish, Spec. Issue Teleost, Fish Immunol. 35 (2011) 1366–1375, https://doi.org/10.1016/j.dci.2011.07.002.

[9] T. Forseth, B.T. Barlaup, B. Finstad, P. Fiske, H. Gjøsæter, M. Falkegård, A. Hindar, T.A. Mo, A.H. Rikardsen, E.B. Thorstad, L.A. Vøllestad, V. Wennevik, The major threats to Atlantic salmon in Norway, ICES J. Mar. Sci. 74 (2017) 1496–1513, https://doi.org/10.1093/icesjms/fsx020.

[10] E. Halttunen, K.-Ø. Gjelland, K.A. Glover, I.A. Johnsen, R.-M. Serra-Llinares, Ø. Skaala, R. Nilsen, P.-A. Bjørn, Ø. Karlsen, B. Finstad, O.T. Skilbrei, Migration of Atlantic salmon post-smolts in a fjord with high infestation pressure of salmon lice, Mar. Ecol. Prog. Ser. 592 (2018) 243–256.

[11] K.W. Vollset, R.I. Krontveit, P.A. Jansen, B. Finstad, B.T. Barlaup, O.T. Skilbrei, M. Krkošek, P. Romunstad, A. Aunsmo, A.J. Jensen, Impacts of parasites on marine survival of Atlantic salmon: a meta-analysis, Fish Fish. 17 (2016) 714–730.

[12] Norwegian Ministry of Fisheries, Regulations on the control of salmon lice in aquaculture facilities, Lovdata, 2012. https://lovdata.no/dokument/SF/forskrift/2012-12-05-1140?q=lakselus. (Accessed 16 April 2024).

[13] O. Torrissen, S. Jones, F. Asche, A. Guttormsen, O.T. Skilbrei, F. Nilsen, T. E. Horsberg, D. Jackson, Salmon lice–impact on wild salmonids and salmon aquaculture, J. Fish. Dis. 36 (2013) 171–194.

[14] S. Bravo, J. Treasurer, The management of the sea lice in Chile: a review, Rev. Aquacult. 15 (2023) 1749–1764, https://doi.org/10.1111/raq.12815.

[15] K. Overton, T. Dempster, F. Oppedal, T.S. Kristiansen, K. Gismervik, L.H. Stien, Salmon lice treatments and salmon mortality in Norwegian aquaculture: a review, Rev. Aquacult. 11 (2019) 1398–1417, https://doi.org/10.1111/raq.12299.

[16] S.C. Johnson, L.J. Albright, The developmental stages of *Lepeophtheirus salmonis* (Krøyer, 1837) (Copepoda: Caligidae), Can. J. Zool. 69 (1991) 929–950, https://doi.org/10.1139/z91-138.

[17] L.A. Hamre, C. Eichner, C.M.A. Caipang, S.T. Dalvin, J.E. Bron, F. Nilsen, G. Boxshall, R. Skern-Mauritzen, The salmon louse *Lepeophtheirus salmonis* (Copepoda: Caligidae) life cycle has only two chalimus stages, PLoS One 8 (2013) e73539, https://doi.org/10.1371/journal.pone.0073539.

[18] J.E. Bron, C. Sommerville, M. Jones, G.H. Rae, The settlement and attachment of early stages of the salmon louse, *Lepeophtheirus salmonis* (Copepoda: Caligidae) on the salmon host, *Salmo salar*, J. Zool. 224 (1991) 201–212, https://doi.org/10.1111/j.1469-7998.1991.tb04799.x.

[19] S. Dalvin, L.v.G. Jørgensen, P.W. Kania, S. Grotmol, K. Buchmann, A.-C. Øvergård, Rainbow trout *Oncorhynchus mykiss* skin responses to salmon louse *Lepeophtheirus salmonis*: from copepodid to adult stage, Fish Shellfish Immunol. 103 (2020) 200–210, https://doi.org/10.1016/j.fsi.2020.05.014.

[20] E.I. Heggland, M. Dondrup, F. Nilsen, C. Eichner, Host gill attachment causes blood-feeding by the salmon louse (*Lepeophtheirus salmonis*) chalimus larvae and alters parasite development and transcriptome, Parasites Vectors 13 (2020) 225, https://doi.org/10.1186/s13071-020-04096-0.

[21] A.-C. Øvergård, L.A. Hamre, S. Grotmol, F. Nilsen, Salmon louse rhabdoviruses: impact on louse development and transcription of selected Atlantic salmon immune genes, Dev. Comp. Immunol. 86 (2018) 86–95, https://doi.org/10.1016/j.dci.2018.04.023.

[22] A.-C. Øvergård, C. Eichner, N. Nuñez-Ortiz, H. Kongshaug, A. Borchel, S. Dalvin, Transcriptomic and targeted immune transcript analyses confirm localized skin immune responses in Atlantic salmon towards the salmon louse, Fish Shellfish Immunol. (2023) 108835, https://doi.org/10.1016/j.fsi.2023.108835.

[23] M.D. Fast, R.W. Neill, A. Mustafa, D.E. Sims, S. Johnson C, G. Conboy, D. Speare, G. Johnson, J.F. Burka, Susceptibility of rainbow trout *Oncorhynchus mykiss*, Atlantic salmon *Salmo salar* and coho salmon *Oncorhynchus kisutch* to experimental infection with sea lice *Lepeophtheirus salmonis*, Dis. Aquat. Organ. 52 (2002) 57–68.

[24] S. Jones, E. Kim, W. Bennett, Early development of resistance to the salmon louse, *Lepeophtheirus salmonis* (Krøyer), in juvenile pink salmon, *Oncorhynchus gorbuscha* (Walbaum), J. Fish. Dis. 31 (2008) 591–600, https://doi.org/10.1111/j.1365-2761.2008.00933.x.

[25] B.J.G. Sutherland, K.W. Koczka, M. Yasuike, S.G. Jantzen, R. Yazawa, B.F. Koop, S. R.M. Jones, Comparative transcriptomics of Atlantic *Salmo salar*, chum *Oncorhynchus keta* and pink salmon *O. gorbuscha* during infections with salmon lice *Lepeophtheirus salmonis*, BMC Genom. 15 (2014), https://doi.org/10.1186/1471-2164-15-200, 200–200.

[26] S.R.M. Jones, M.D. Fast, S.C. Johnson, D.B. Groman, Differential rejection of salmon lice by pink and chum salmon: disease consequences and expression of proinflammatory genes, Dis. Aquat. Organ. 75 (2007) 229–238.

[27] S. Johnson, L. Albright, Comparative susceptibility and histopathology of the response of naive atlantic, chinook and coho salmon to experimental-infection with *Lepeophtheirus salmonis* (Copepoda, Caligidae), Dis. Aquat. Organ. 14 (1992) 179–193, https://doi.org/10.3354/dao014179.

[28] L.M. Braden, D. Michaud, D. Groman, P. Byrne, T.S. Hori, M.D. Fast, Rejection of *Lepeophtheirus salmonis* driven in part by chitin sensing is not impacted by seawater acclimitization in Coho salmon (*Oncorhynchus kisutch*), Sci. Rep. 13 (2023) 9685, https://doi.org/10.1038/s41598-023-36632-0.

[29] H.M.D. Midtbø, C. Eichner, L.A. Hamre, M. Dondrup, L. Flesland, K.H. Tysseland, H. Kongshaug, A. Borchel, R.H. Skoge, F. Nilsen, A.-C. Øvergård, Salmon louse labial gland enzymes: implications for host settlement and immune modulation, Front. Genet. 14 (2024). https://www.frontiersin.org/articles/10.3389/fgene.2023.1303898.

[30] A.-C. Øvergård, H.M.D. Midtbø, L.A. Hamre, M. Dondrup, G.E.K. Bjerga, Ø. Larsen, J.K. Chettri, K. Buchmann, F. Nilsen, S. Grotmol, Small, charged proteins in salmon louse (*Lepeophtheirus salmonis*) secretions modulate Atlantic salmon (*Salmo salar*) immune responses and coagulation, Sci. Rep. 12 (2022) 7995, https://doi.org/10.1038/s41598-022-11773-w.

[31] Z. Kabata, Mouth and mode of feeding of Caligidae (Copepoda), parasites of fishes, as determined by light and scanning electron microscopy, J. Fish. Res. Board Can. 31 (1974) 1583–1588, https://doi.org/10.1139/f74-199.

[32] A.-C. Øvergård, L.A. Hamre, E. Harasimczuk, S. Dalvin, F. Nilsen, S. Grotmol, Exocrine glands of *Lepeophtheirus salmonis* (Copepoda: Caligidae): distribution, developmental appearance, and site of secretion, J. Morphol. 277 (2016) 1616–1630, https://doi.org/10.1002/jmor.20611.

[33] G. Sridharan, A.A. Shankar, Toluidine blue: a review of its chemistry and clinical utility, J. Oral Maxillofac. Pathol. 16 (2012). https://journals.lww.com/jpat/fulltext/2012/16020/toluidine_blue_a_review_of_its_chemistry_and.17.aspx.

[34] C. Eichner, F. Nilsen, S. Grotmol, S. Dalvin, A method for stable gene knock-down by RNA interference in larvae of the salmon louse (*Lepeophtheirus salmonis*), Exp. Parasitol. 140 (2014) 44–51.

[35] L.A. Hamre, F. Nilsen, Individual fish tank arrays in studies of *Lepeophtheirus salmonis* and lice loss variability, Dis. Aquat. Organ. 97 (2011) 47–56.

[36] A.-C. Øvergård, A.H. Nerland, S. Patel, Evaluation of potential reference genes for real time RT-PCR studies in Atlantic halibut (*Hippoglossus Hippoglossus* L.); during development, in tissues of healthy and NNV-injected fish, and in anterior kidney leucocytes, BMC Mol. Biol. 11 (2010) 1–15.

[37] R. Patro, G. Duggal, M.I. Love, R.A. Irizarry, C. Kingsford, Salmon provides fast and bias-aware quantification of transcript expression, Nat. Methods 14 (2017) 417–419.

[38] The Galaxy Community, The Galaxy platform for accessible, reproducible and collaborative biomedical analyses: 2022 update, Nucleic Acids Res. 50 (2022) W345–W351.

[39] F.J. Martin, M.R. Amode, A. Aneja, O. Austine-Orimoloye, A.G. Azov, I. Barnes, A. Becker, R. Bennett, A. Berry, J. Bhai, Ensembl 2023, Nucleic Acids Res. 51 (2023) D933–D941.

[40] A.D. Yates, J. Allen, R.M. Amode, A.G. Azov, M. Barba, A. Becerra, J. Bhai, L. I. Campbell, M. Carbajo Martinez, M. Chakiachvili, Ensembl Genomes 2022: an expanding genome resource for non-vertebrates, Nucleic Acids Res. 50 (2022) D996–D1003.

[41] R Core Team, R: A Language and Environment for Statistical Computing, R Foundation for Statistical Computing, 2013. No Title.

[42] M.I. Love, W. Huber, S. Anders, Moderated estimation of fold change and dispersion for RNA-seq data with DESeq2, Genome Biol. 15 (2014) 1–21.

[43] C. Soneson, M. Love, M. Robinson, Differential analyses for RNA-seq: transcript-level estimates improve gene-level inferences [version 2; peer review: 2 approved], F1000Research 4 (2016), https://doi.org/10.12688/f1000research.7563.2.

[44] A. Zhu, J.G. Ibrahim, M.I. Love, Heavy-tailed prior distributions for sequence count data: removing the noise and preserving large differences, Bioinformatics 35 (2019) 2084–2092.

[45] F.E. Pettersen, I. Fyllingen, A. Kavlie, N.P. Maaseide, J. Glette, C. Endresen, H. I. Wergeland, Monoclonal antibodies reactive with serum IgM and leukocytes from Atlantic salmon (*Salmo salar* L.), Fish Shellfish Immunol. 5 (1995) 275–287, https://doi.org/10.1006/fsim.1995.0027.

[46] J. Jumper, R. Evans, A. Pritzel, T. Green, M. Figurnov, O. Ronneberger, K. Tunyasuvunakool, R. Bates, A. Žídek, A. Potapenko, A. Bridgland, C. Meyer, S.A. A. Kohl, A.J. Ballard, A. Cowie, B. Romera-Paredes, S. Nikolov, R. Jain, J. Adler, T. Back, S. Petersen, D. Reiman, E. Clancy, M. Zielinski, M. Steinegger, M. Pacholska, T. Berghammer, S. Bodenstein, D. Silver, O. Vinyals, A.W. Senior, K. Kavukcuoglu, P. Kohli, D. Hassabis, Highly accurate protein structure prediction with AlphaFold, Nature 596 (2021) 583–589, https://doi.org/10.1038/s41586-021-03819-2.

[47] A.R. Poh, R.J.J. O'Donoghue, M. Ernst, Hematopoietic cell kinase (HCK) as a therapeutic target in immune and cancer cells, Oncotarget 6 (2015). https://www.oncotarget.com/article/4199/text/.

[48] B. Myrnes, M. Seppola, A. Johansen, K. Øverbø, L. Callewaert, L. Vanderkelen, C. W. Michiels, I.W. Nilsen, Enzyme characterisation and gene expression profiling of Atlantic salmon chicken- and goose-type lysozymes, Dev. Comp. Immunol. 40 (2013) 11–19, https://doi.org/10.1016/j.dci.2013.01.010.
[49] S.M. Paulsen, R.E. Engstad, B. Robertsen, Enhanced lysozyme production in Atlantic salmon (*Salmo salar* L.) macrophages treated with yeast β-glucan and bacterial lipopolysaccharide, Fish Shellfish Immunol. 11 (2001) 23–37, https://doi.org/10.1006/fsim.2000.0291.
[50] L. Callewaert, C.W. Michiels, Lysozymes in the animal kingdom, J. Biosci. 35 (2010) 127–160.
[51] S.A. Ragland, A.K. Criss, From bacterial killing to immune modulation: recent insights into the functions of lysozyme, PLoS Pathog. 13 (2017) e1006512, https://doi.org/10.1371/journal.ppat.1006512.
[52] Z. Zhu, T. Zheng, R.J. Homer, Y.-K. Kim, N.Y. Chen, L. Cohn, Q. Hamid, J.A. Elias, Acidic mammalian chitinase in asthmatic Th2 inflammation and IL-13 pathway activation, Science 304 (2004) 1678–1682, https://doi.org/10.1126/science.1095336.
[53] D. Hartl, C.H. He, B. Koller, C.A.D. Silva, R. Homer, C.G. Lee, J.A. Elias, Acidic mammalian chitinase is secreted via an ADAM17/epidermal growth factor receptor-dependent pathway and stimulates chemokine production by pulmonary epithelial cells, J. Biol. Chem. 283 (2008) 33472–33482, https://doi.org/10.1074/jbc.M805574200.
[54] L. Shuhui, Y.-K. Mok, W.S.F. Wong, Role of mammalian chitinases in asthma, Int. Arch. Allergy Immunol. 149 (2009) 369–377, https://doi.org/10.1159/000205583.
[55] B.J. Sutherland, S.G. Jantzen, D.S. Sanderson, B.F. Koop, S.R. Jones, Differentiating size-dependent responses of juvenile pink salmon (*Oncorhynchus gorbuscha*) to sea lice (*Lepeophtheirus salmonis*) infections, Comp. Biochem. Physiol., Part D: Genomics Proteomics 6 (2011) 213–223.
[56] E. Elinav, T. Strowig, J. Henao-Mejia, R.A. Flavell, Regulation of the antimicrobial response by NLR proteins, Immunity 34 (2011) 665–679.
[57] T.F. Robertson, Y. Hou, J. Schrope, S. Shen, J. Rindy, J.-D. Sauer, H.Q. Dinh, A. Huttenlocher, A tessellated lymphoid network provides whole-body T cell surveillance in zebrafish, Proc. Natl. Acad. Sci. USA 120 (2023) e2301137120, https://doi.org/10.1073/pnas.2301137120.
[58] H. Holm, N. Santi, S. Kjøglum, N. Perisic, S. Skugor, Ø. Evensen, Difference in skin immune responses to infection with salmon louse (*Lepeophtheirus salmonis*) in Atlantic salmon (*Salmo salar* L.) of families selected for resistance and susceptibility, Fish Shellfish Immunol. 42 (2015) 384–394, https://doi.org/10.1016/j.fsi.2014.10.038.
[59] M.S. Ugelvik, S. Dalvin, The effect of different intensities of the ectoparasitic salmon lice (*Lepeophtheirus salmonis*) on Atlantic salmon (*Salmo salar*), J. Fish. Dis. 45 (2022) 1133–1147, https://doi.org/10.1111/jfd.13649.
[60] S. Bui, P.G. Fjelldal, M. Hvas, Ø. Karlsen, S. Dalvin, Louse-induced mortality thresholds in Atlantic salmon of wild-origin, Conserv. Sci. Pract. 6 (2024) e13079, https://doi.org/10.1111/csp2.13079.
[61] S. Bui, F. Oppedal, V. Nola, L.T. Barrett, Where art thou louse? A snapshot of attachment location preferences in salmon lice on Atlantic salmon hosts in sea cages, J. Fish. Dis. 43 (2020) 697–706, https://doi.org/10.1111/jfd.13167.
[62] C.D. Todd, A.M. Walker, J.E. Hoyle, S.J. Northcott, A.F. Walker, M.G. Ritchie, Infestations of wild adult Atlantic salmon (*Salmo salar* L.) by the ectoparasitic copepod sea louse *Lepeophtheirus salmonis* Krøyer: prevalence, intensity and the spatial distribution of males and [2pt] females on the host fish, Hydrobiologia 429 (2000) 181–196, https://doi.org/10.1023/A:1004031318505.
[63] D. Chauhan, E. Bartok, M.M. Gaidt, F.J. Bock, J. Herrmann, J.M. Seeger, P. Broz, R. Beckmann, H. Kashkar, S.W. Tait, BAX/BAK-induced apoptosis results in caspase-8-dependent IL-1β maturation in macrophages, Cell Rep. 25 (2018) 2354–2368.
[64] B. Moon, S. Yang, H. Moon, J. Lee, D. Park, After cell death: the molecular machinery of efferocytosis, Exp. Mol. Med. 55 (2023) 1644–1651, https://doi.org/10.1038/s12276-023-01070-5.
[65] G.K. Atkin-Smith, R. Tixeira, S. Paone, S. Mathivanan, C. Collins, M. Liem, K. J. Goodall, K.S. Ravichandran, M.D. Hulett, I.K.H. Poon, A novel mechanism of generating extracellular vesicles during apoptosis via a beads-on-a-string membrane structure, Nat. Commun. 6 (2015) 7439, https://doi.org/10.1038/ncomms8439.
[66] J.F. Kerr, A.H. Wyllie, A.R. Currie, Apoptosis: a basic biological phenomenon with wideranging implications in tissue kinetics, Br. J. Cancer 26 (1972) 239–257.
[67] I.K.H. Poon, Y.-H. Chiu, A.J. Armstrong, J.M. Kinchen, I.J. Juncadella, D.A. Bayliss, K.S. Ravichandran, Unexpected link between an antibiotic, pannexin channels and apoptosis, Nature 507 (2014) 329–334, https://doi.org/10.1038/nature13147.
[68] R. Tixeira, S. Caruso, S. Paone, A.A. Baxter, G.K. Atkin-Smith, M.D. Hulett, I. K. Poon, Defining the morphologic features and products of cell disassembly during apoptosis, Apoptosis 22 (2017) 475–477.
[69] S. Caruso, G.K. Atkin-Smith, A.A. Baxter, R. Tixeira, L. Jiang, D.C. Ozkocak, J. P. Santavanond, M.D. Hulett, P. Lock, T.K. Phan, I.K.H. Poon, Defining the role of cytoskeletal components in the formation of apoptopodia and apoptotic bodies during apoptosis, Apoptosis 24 (2019) 862–877, https://doi.org/10.1007/s10495-019-01565-5.
[70] A.J. Legrand, M. Konstantinou, E.F. Goode, P. Meier, The diversification of cell death and immunity: memento mori, Mol. Cell 76 (2019) 232–242, https://doi.org/10.1016/j.molcel.2019.09.006.
[71] J.M.O. Fernandes, G.D. Kemp, M.G. Molle, V.J. Smith, Anti-microbial properties of histone H2A from skin secretions of rainbow trout, *Oncorhynchus mykiss*, Biochem. J. 368 (2002) 611–620, https://doi.org/10.1042/bj20020980.
[72] T.W.R. Halverson, M. Wilton, K.K.H. Poon, B. Petri, S. Lewenza, DNA is an antimicrobial component of neutrophil extracellular traps, PLoS Pathog. 11 (2015) e1004593, https://doi.org/10.1371/journal.ppat.1004593.
[73] A.P. Van, N. Álvarez de Haro, J.E. Bron, A.P. Desbois, Chromatin extracellular trap release in rainbow trout, *Oncorhynchus mykiss* (Walbaum, 1792), Fish Shellfish Immunol. 99 (2020) 227–238, https://doi.org/10.1016/j.fsi.2020.01.040.
[74] T.A. Fuchs, U. Abed, C. Goosmann, R. Hurwitz, I. Schulze, V. Wahn, Y. Weinrauch, V. Brinkmann, A. Zychlinsky, Novel cell death program leads to neutrophil extracellular traps, J. Cell Biol. 176 (2007) 231–241, https://doi.org/10.1083/jcb.200606027.
[75] N. Álvarez de Haro, A.P. Van, C.T. Robb, A.G. Rossi, A.P. Desbois, Release of chromatin extracellular traps by phagocytes of Atlantic salmon, *Salmo salar* (Linnaeus, 1758), Fish Shellfish Immunol. 119 (2021) 209–219, https://doi.org/10.1016/j.fsi.2021.08.023.
[76] H.R. Thiam, S.L. Wong, D.D. Wagner, C.M. Waterman, Cellular mechanisms of NETosis, Annu. Rev. Cell Dev. Biol. 36 (2020) 191–218, https://doi.org/10.1146/annurev-cellbio-020520-111016.
[77] G. Sollberger, D.O. Tilley, A. Zychlinsky, Neutrophil extracellular traps: the biology of chromatin externalization, Dev. Cell 44 (2018) 542–553, https://doi.org/10.1016/j.devcel.2018.01.019.
[78] K.L. Rock, H. Kono, The inflammatory response to cell death, Annu. Rev. Pathol. 3 (2008) 99–126, https://doi.org/10.1146/annurev.pathmechdis.3.121806.151456.